



Gridded Emissions of Air Pollutants for the period 1970-2012 within EDGAR v4.3.2

Monica Crippa¹, Diego Guizzardi², Marilena Muntean¹, Edwin Schaaf¹, Frank Dentener¹, John A. van Aardenne³, Suvi Monni⁴, Ulrike Doering⁵, Jos G. J Olivier⁶,
5 Valerio Pagliari¹, Greet Janssens-Maenhout¹

¹European Commission, Joint Research Centre (JRC), Via E. Fermi 2749, I-21027 Ispra (VA), Italy

²Didesk Informatica, Verbania, Italy

³European Environment Agency, Copenhagen, Denmark

10 ⁴Benviroc Ltd., Helsinki, Finland

⁵Umweltbundesamt, Dessau, Germany

⁶PBL Netherlands Environmental Assessment Bureau, Den Hague, The Netherlands

Correspondence to: M. Crippa (monica.crippa@ec.europa.eu)

15 **Abstract** The new version v4.3.2 of the Emissions Database for Global Atmospheric Research (EDGAR v4.3.2) compiles gaseous and particulate air pollutant emissions, making use of the same anthropogenic sectors, time period (1970-2012) and international activity data as used for estimating GHG emissions as described in a companion paper (Janssens-Maenhout et al., 2017). All human activities, except large scale biomass burning and land use, land-use
20 change and forestry, are included in the emissions calculation. The bottom-up compilation methodology of sector-specific emissions was applied consistently for all world countries, providing methodological transparency and comparability between countries. In addition to the activity data used to estimate GHG emissions, air pollutant emissions are determined by the process technology and end-of-pipe emission reduction abatements. Region-specific
25 emission factors and abatement measures were selected from recent scientific available literature and reports. Compared to previous versions of EDGAR, the EDGAR v4.3.2 dataset covers all gaseous and particulate air pollutants, has extended time series (1970-2012) and has been evaluated with QC/QA procedures both for the emission time series (e.g. PM mass balance, gap-filling for missing data, split-up of countries over time, etc.) and gridmaps (full
30 coverage of the world, complete mapping of EDGAR emissions with sector-specific proxies, etc.). This publication focuses on the gaseous air pollutants of CO, NO_x, SO₂, total NMVOC and NH₃ and on the aerosols PM₁₀, PM_{2.5}, BC and OC. Considering the 1970-2012 time period, global emissions of SO₂ increased from 99 to 103 Tg, CO from 441 to 562 Tg, NO_x from 68 to 122 Tg, NMVOC from 119 to 170 Tg, NH₃ from 25 to 59 Tg, PM₁₀ from 37 to 65
35 Tg, PM_{2.5} from 24 to 41 Tg, BC from 2.7 to 4.5 Tg and OC from 9 to 11 Tg. We present the country-specific emission totals and analyse the larger emitting countries (including the European Union), to provide insights on major sector contributions. In addition, per capita and



per GDP emissions and implied emission factors - the apparent emissions per unit of production or energy consumption are presented. We find that the implied EFs are higher for low income countries compared to high income countries, but in both cases decreasing from 1970 to 2012. The comparison with other global inventories, such as HTAP v2.2 and CEDS, reveals insights on the uncertainties as well as the impact of data revisions (e.g. activity data, emission factors, etc.). As an additional metric we analyse the emission ratios of some pollutants to CO₂ (e.g. CO/CO₂, NO_x/CO₂, NO_x/CO and SO₂/CO₂) by sector, region and time to identify any decoupling of air pollutant emissions from energy production activities and to demonstrate the potential of such ratios to compare to satellite derived emission data. Gridded emissions are also made available for the 1970-2012 historic time series, disaggregated for 26 anthropogenic sectors using updated spatial proxies. The analysis of the evolution of hot spots over time allowed us to identify areas with growing emissions and where emissions should be constrained to improve global air quality (e.g. China, India, Middle East and some Southern American countries are often characterized by high emitting areas which are changing rapidly compared to Europe or USA where stable or decreasing emissions are evaluated). Sector-and component specific contributions to gridcell emissions may help the modelling and satellite communities to disaggregate atmospheric column amounts and concentrations into main emitting sectors. This work addresses not only the emission inventory and modelling communities, but also aims to broaden the usefulness information available in a global emission inventory such as EDGAR to also include the measurement community. Data are publicly available online through the EDGAR website http://edgar.jrc.ec.europa.eu/overview.php?v=432_AP&SECURE=123 and registered under DOI: https://data.europa.eu/doi/10.2904/JRC_DATASET_EDGAR.

25 Introduction

Air pollutant emissions represent a major concern for air quality (Monks et al., 2009), climate impacts (Anenmber et al., 2012; IPCC, 2013), health (WHO, 2016) and environmental effects (van Dingenen et al., 2009) and visibility (Wang et al., 2012). The first international treaty dealing with air quality was the UNECE Convention on Long-Range Transboundary Air Pollution (CLRTAP) which entered into force in 1979 with focus on global, regional and local air quality issues and acid rain (<https://www.unece.org>). Atmospheric pollutants can be emitted as gaseous compounds, e.g. SO₂, NO_x, CO, NMVOC (non-methane volatile organic compounds), NH₃, etc., or as particles with different size and composition, e.g. particulate matter with diameter less than 10, 2.5 and 1 μm (PM₁₀, PM_{2.5} and PM₁, respectively), black carbon (BC) and organic carbon (OC). These pollutants can be directly injected in the atmosphere by anthropogenic or natural sources (primary emissions) or they can form through secondary chemical-physical processes (secondary components). The aforementioned gaseous compounds consists of primary pollutants together with primarily emitted particulate matter, while the secondary components mainly include secondary organic (SOA) and inorganic aerosols (e.g. ammonium nitrates and ammonium sulphates) and ozone (O₃) (Seinfeld and Pandis, 2006). In addition, air pollutants can be transported far away from source regions depending on the pollutants life time, reactivity as well as meteorological dynamics (Maas et



al., 2016). Air pollution sources impact air quality at local, regional and global scales (HTAP, 2010). Moreover, despite regional variations, air pollution is also a ubiquitous problem with to a large extent common solutions between regions. To tackle these regional and global aspects, global emission inventories coupled to chemical transport models (CTMs) are useful tools, complementing air pollution measurements which provide information on local and regional air quality impacts. In the latest years several global emission inventories have been developed, such as the one of Lamarque et al. (2010), the MACCity by Granier et al. (2011), the one documented by Klimont et al. (2013) for SO₂, the HTAP_v2.2 by Janssens-Maenhout et al. (2015), the Community Emission Data System (CEDS) by Hoesly et al. (2017) and the GAINS-based inventory named ECLIPSEV5a by Klimont et al. (2017) for particulate matter. The EDGAR database (Emissions Database for Global Atmospheric Research) is a bottom-up global database providing historic emission time series and gridmaps for all countries from 1970 till nowadays for both air pollutants and greenhouse gases calculated in a consistent and transparent way and therefore allowing comparability amongst countries. The work presented here is complementary to the study on the greenhouse gases by Janssens-Maenhout et al. (2017) and aims at the documenting the new EDGAR v4.3.2 version with focus on the gaseous air pollutants (SO₂, NO_x, CO, NMVOC and NH₃) and on the aerosols (PM₁₀, PM_{2.5} distinguishing between the bio and fossil components, BC (to be interpreted as EC) and OC). The purpose of this publication is to document the methodology and the data availability of the EDGAR v4.3.2 air pollutants release. A huge amount of information is included in this release, covering 42 years data, 26 aggregated emission sectors, 226 countries and 9 substances. In addition, emissions are represented both as time series and emission gridmaps. A detailed analysis of all driving data, trends and peculiarities of this dataset is beyond the scope of this work, Instead we focus on presenting the key-outcomes of regional and global emissions and their temporal trends. We also provide an analysis of some key-futures of the large amount of information available at grid cell level, such as the sector relative contribution or the emission change over time of the different pollutants and sectors, which warrant further analysis by modelling and satellite communities. In addition we examine for countries and sector the per capita and per GDP emissions, implied emission factors, etc. to analyse regional differences in equity and efficiency. In Sect. 2 we describe the EDGAR methodology, in addition to the extensive documentation provided in the companion paper on GHGs (Janssens-Maenhout et al., 2017); then in Sect. 3, we show the global trends and the comparison with other global inventories, such as HTAP v2.2 and CEDS revealing insights on the causes of uncertainty and the impact of data revisions. Compared to the previous EDGAR v4.3.1 release, the current EDGAR v4.3.2 dataset covers a longer time series (1970-2012 vs. 1970-2010), some updates in the activity data and emission factors, full quality assurance and quality check procedure implementation, but it covers the same pollutants and it relies on the same proxy data as used in v4.3.1 (Crippa et al., 2016a). In Sect. 4 we present implied emission factors (apparent EFs per unit of production or energy consumption), per capita and per GDP emissions, as well as country-specific emission totals amongst world countries. We also analyse the variations of several large emitting countries and the EU in more depth, to provide insights on the main sectors contributing to the emissions of each pollutant. Finally, in Sections 5 and 6 we discuss the sector-specific relative composition at gridcell level and



analyse the emission ratios of CO/CO₂, NO_x/CO₂ and SO₂/CO₂ by sector, region and time, providing useful information for the measurements community. In addition we provide sector-specific emission shares calculated at gridcell level with 0.1°x0.1° resolution allowing the retrieval of sectorial information from the total column measurements of each pollutant. Data are presented online for each source category with annual and monthly global emissions gridmaps at 0.1°x0.1° resolution. All data can be freely accessed via the EDGAR website http://edgar.jrc.ec.europa.eu/overview.php?v=432_AP&SECURE=123 and they are registered under DOI: https://data.europa.eu/doi/10.2904/JRC_DATASET_EDGAR.

1 Methods

10 2.1 Methodology of the bottom-up emission inventory compilation and distribution

The EDGAR v4.3.2 air pollutant dataset incorporates a full differentiation of emission processes with technology-specific emission factors and additional end-of-pipe abatement measures, which are more relevant for air pollutants than for greenhouse gases. The definition of the anthropogenic emission sectors was kept identical to the ones used for the EDGAR v4.3.2 GHG dataset (Janssens-Maenhout et al., 2017), based on the IPCC (1996) guidelines, for which the conversion to the Selected Nomenclature for Sources of Air Pollution (SNAP) categories used by TFEIP and the parties of the LRTAP is unambiguously given¹. The same time period and the same international activity data as for the GHGs are also used for consistency. The equation for GHG emissions is modified by a factor f that specifies the components of each pollutant, e.g. gaseous NMVOCs (Huang et al., 2017; http://edgar.jrc.ec.europa.eu/overview.php?v=432_VOC_spec), particulate OC, NO_x (sum of NO and NO₂), etc.:

$$EM_i(C, t, x) = \sum_{j,k} \left[AD_i(C, t) * TECH_{i,j}(C, t) * EOP_{i,j,k}(C, t) * EF_{i,j}(C, t, x) * (1 - RED_{i,j,k}(C, t, x)) * f_x \right] \quad (1)$$

with emissions (EM) from a given sector i in a country C accumulated during a year t for a chemical compound x with the country-specific activity data (AD), quantifying the human activity for sector i , with the mix of j technologies (TECH) and with the mix of k (end-of-pipe) abatement measures (EOP) installed with share k for each technology j , and with the uncontrolled emission factor (EF) for each sector i and technology j with relative reduction (RED) by abatement measure k . As discussed in the next section, the uncontrolled emission factors and abatement measures were applied at Tier1 to Tier3 level depending on the anthropogenic sector.

Most emissions are computed using international activity data from IEA (2014), FAOSTAT (2016a, 2016b), USGS (2014), UN STATS (2014), UNFCCC (2014), similar to the GHG emission dataset described by Janssens-Maenhout et al. (2017) and references therein). These

¹ http://www.ceip.at/fileadmin/inhalte/emep/pdf/NFR09_SNAP_GNFR.pdf; accessed March 2018



data are complemented with national or regional information on the technology mixes and end-of-pipe measures and using the latest available scientific knowledge on the emission factors, mostly based on the EMEP/EEA (2013) guidebook. A new version of the EMEP/EEA guidebook (2016) has been recently released with significant updates for the emission factors (in particular for the agricultural sector); however, these updates are not included in the current release of EDGAR v4.3.2. The details of EDGAR v4.3.2 activity data sources (i.e. the population, energy, fossil fuel production, industrial processes, solvents, agricultural, solid waste product, wastewater and other historical statistics) are given in section 2.3 of Janssens-Maenhout et al. (2017).

10 For the spatial and temporal distribution of the sector-specific emission totals of a substance x for a country C in the year t (monthly) and space (on $0.1^\circ \times 0.1^\circ$ grids, defined with bottom-left corner for each cell) the same allocation algorithm and proxy datasets used for the GHG dataset of Janssens-Maenhout et al. (2017) are applied (Table S4a of the aforementioned paper is also reported in Table S7 of the supplementary material). The temporal profiles and
15 the geospatial proxy data are described in Sections 2.4 and 2.5 of Janssens-Maenhout et al. (2017), respectively. In the following, we will describe our results looking at aggregated sectors: energy (power generation sector), industry (including industrial combustion, production of chemicals, non-metallic minerals, non-ferrous metals, iron and steel, solvents, food, paper, non-energy use of fuels, fuel production and transformation, refineries and fossil
20 fuel fires), transport (including both road and non- road transport), residential (including both domestic combustion and waste disposal), agriculture (including agricultural soils, agricultural waste burning and manure management).

2.2 Data sources to model the technology-based emission process

The emissions cover all human-induced activities, except large scale biomass burning and
25 activities of land use, land-use change and Forestry from 1970-2012. The bottom-up compilation of sector-specific emissions was applied consistently for all world countries, providing methodological transparency and comparability amongst countries. In addition to the activity data, the air pollutant emissions are determined by the technology and end-of-pipe abatements (contrary to GHGs). Region-specific emission factors and abatement measures
30 were selected from latest available literature and available recent knowledge. Section S4 of the supplementary materials provides an overview of the technologies and abatements implemented in EDGAR v4.3.2 for all sectors. Combustion technologies, combustion temperatures and the end-of-pipe measures determine the amount of air pollutants emitted and are modelled separately for stationary and mobile combustion sources. Under the latter, the
35 road transport sector is modelled with pre-EURO till EURO 5 standards, US Tier 1 till Tier 3 standards and described in detail in Crippa et al. (2016b), whereas the aviation sector is modelled following Eyers et al. (2005) and the shipping sector follows Dalsoeren et al. (2009).

40 The stationary combustion sector includes small, medium large boilers for gas/liquid fuels, internal combustion engines, gas turbines, fluidized bed, grate firing, and pulverized coal dry bottom boilers. Country-specific shares of the technologies are taken from the UCI Platts



Power Plant Database (2008) and updated with region specific information from the EPRTR v4.2 database for Europe and with information of Zhao et al. (2012) for China, as documented in Muntean et al. (2018). Further updates of the technologies used in this sector are foreseen for next releases of the EDGAR database. The end-of-pipe measures are from the IEA Clean Coal Centre (IEA Clean coal power DB, 2008, <http://www.iea-coal.co.uk/>), updated with EPRTR (2012) for Europe, EPA (2014) for USA, Zhao et al. (2012) for China and countries falling short in data the technology mixes and end-of-pipe measures are estimated using neighbouring countries or regions as proxy. For USA, EU and China, air quality policies are assumed to kick in with immediate and full effectiveness, so possible phased implementation imposed by these policies in which regulations have to be implemented is not considered in our database. In Europe policies include in particular the National Emission Ceiling directive (2001/81/EC), but also the earlier air quality directives (80/779/EEC, 85/203/EEC), the air quality framework directive (96/62/EC), the ambient air directive (2000/69/EC for CO), the ambient air quality directive (2008/50/EC) mainly for PM and the IPPC directive (2008/1/EC). The 2016 revision of the National Emission Ceilings Directive, effective from 2020 onwards, falls outside the considered time period. For the energy sector end-of-pipe measures for particulate matter components are applied, specifically cyclones (with 90% abatement for PM₁₀ and 0% for PM_{2.5} and its carbonaceous components), combinations of electrostatic precipitators and fabric filters (with 99.95% abatement for PM₁₀ and from 98.3 to 99.6% for PM_{2.5} and its components). The aforementioned abatements are applied to all fuels, in particular to coal-related ones. SO_x reduction measures of 50% by non-regenerative-dry (dry FGD) and SO_x reduction of 90% by non-regenerative semidry, non-regenerative wet (wet flue gas desulfurization (FGD)) and regenerative SO_xNO_x are also included. Concerning NO_x reduction measures, 30% reduction is assumed for low-NO_x burners, low excess air, air staging in furnace, flue gas recirculation - in furnace, reduced air preheat, fuel staging, a reduction of 60% for selective catalytic reduction, and of 90% for selective catalytic reduction combined with combustion modification; NO_x reduction from 30% to 90% is obtained by selective non-catalytic reduction and of 90% by SO_xNO_x combined measures. For these point sources, data from the EPRTRv4.2 has been consulted as well as the reported specifications under the large combustion directive.

For the transport sector, a description is given by Crippa et al. (2016b). We did not consider cold starts, superemitting vehicles, resuspension of road dust and brake and tyre wear. In addition, we did use the recommended EF factors for NO_x from test benches instead of from real driving mode measurements. This explains the expected underestimation (with almost factor 2) of the PM_{2.5} emissions and of the NO_x emissions. For the residential sector, we used generic data of few national statistics on e.g. the combustion technology used in the given country, which was also inherited for neighbouring countries in case data was missing.

The data sources for the management systems applied for coal mining (surface or underground, with or without recovery), the technologies for iron & steel production (open hearth furnace, blast oxygen furnace, electric arc furnace), and for the Aluminium smelters (Prebake or Soederberg types), from high to low pressure technologies for the nitric acid production, and the different sewing types for domestic and industrial wastewater treatment



are described in the v4.3.2 GHG companion paper of Janssens-Maenhout et al. (2017). That paper also provides a description of activity data relevant to agricultural emissions: the manure management systems (burned for fuel, dropped in pasture/range/paddock, digester, drylot, daily spread, lagoon, liquid slurry, pit, solid storage or other) and the 4 ecology types for rice cultivation (from rainfed, irrigated, deep water and upland), as these are also determining the CH₄ emission factors.

3 Gaseous and particulate air pollutant emission trends and uncertainty

3.1 Global and regional trends of gaseous and particulate air pollutants emissions

As further discussed in paragraph 3.2 showing the global anthropogenic emission time series of gaseous pollutants and aerosols of EDGAR v4.3.2, over the period 1970-2012, we estimate global increasing emissions for all pollutants, for SO₂ emissions from 99 to 103 Tg, CO from 441 to 562 Tg, NO_x from 68 to 122 Tg, NMVOC from 110 to 170 Tg, NH₃ from 25 to 59 Tg, PM₁₀ from 37 to 65 Tg, PM_{2.5} from 24 to 41 Tg, BC from 2.7 to 4.5 Tg and OC from 9 to 11 Tg. However, significant differences are found in the regional emission trends over 1970-2012 and the corresponding sector shares. In the following, we will mainly focus on the emission trends of some representative gases e.g. SO₂, CO, NO_x and on PM_{2.5} as representative for the aerosol components. Figures 1-4 show the emission gridmaps for the main air pollutants (SO₂, NO_x, CO) and aerosols (PM_{2.5}) in 1970 and 2012, together with the relative sector contribution for major world regions. Sectors have been aggregated as following: energy (power industry), industry and processes (including industrial combustion and all industrial processes), transport (including both road transport and non-road transport), residential (small scale combustion and waste treatment) and agriculture. In 1970, SO₂ emissions were mainly occurring over USA (26 kton) and Europe (28 kton) from the energy, industry and residential sectors, while in 2012 the major emitters were China (32 kton) and India (12 kton) due to the combustion of coal related fuels both in power and non-power industry, in addition to USA (8.2 kton) and Europe (6.6 kton). CO emissions in 1970 were dominated by the contribution of USA (100 kton), Europe (68 kton) and China (54 kton) from the incomplete combustion occurring mainly in the transport and residential sectors, while in 2012 the top emitters were the emerging economies of China (120 kton), Africa (88 kton), India (87 kton) and Latin America (73kton) mainly due to the contribution of household combustion, industrial activities and partly from agricultural waste burning (mainly in Latin America and India). Differently from CO, NO_x emissions result from high-temperature temperature combustion processes, so they are also emitted by power plants and by the transport sector. In 1970, top emitting regions were USA (19 kton) and Europe (14 kton), while in 2012 they were China (30 kton), India (11 kton), Latin America (9.7 kton) and Africa (5.5 kton). Emissions from USA and Europe were slightly decreasing over the considered time period. Finally, PM_{2.5} and the other aerosol components are emitted mainly by small-scale combustion and agricultural waste burning activities. In 1970, both industrialized countries like USA (2.6 kton) and EU (3.6 kton) and emerging economies (China -4.7 kton, India -3.0 kton), Africa (2.4 kton)) represented the top emitting regions, while in 2012 a



significant increasing trend is found mainly for Africa (up to 7.4 kton), India (up to 5.7 kton) and Latin America (up to 3.9 kton). A decreasing trend is estimated for all the other regions, in particular for Europe (1.5 kton), USA (1.3 kton) and China (1.2 kton) reaching less than half of the corresponding 1970 PM_{2.5} emissions.

5

3.2 Comparison of the EDGAR v4.3.2 timeseries with other global inventories

Figures 5a and 5b show the comparison of global anthropogenic emission time series of gaseous pollutants and aerosols as estimated by the different versions of the EDGAR database (EDGAR v4.2 (EC-JRC/PBL, 2011; <http://edgar.jrc.ec.europa.eu/overview.php?v=42>; DOI:10.2904/EDGARv4.2), EDGAR v4.3.1 (Crippa et al., (2016a) and <http://edgar.jrc.ec.europa.eu/overview.php?v=431>; DOI=10.2904/JRC_DATASET_EDGAR) and EDGAR v4.3.2) and several other global inventories such as HTAP_v2.2 (Janssens-Maenhout et al., 2015), MACCity (Granier et al., 2011), CEDS (Hoesly et al., 2017), ECLIPSEV5a (Klimont et al., 2017), the one of Lamarque et al. (2010) and Klimont et al. (2013). Note that not all global inventories cover all pollutants and time series. The comparison of different emission inventories allows us to explore the range of global emission estimates and to identify for which pollutants the emissions show larger discrepancies. For the aerosols, a region- and sector-specific comparison between EDGAR v4.3.2 and ECLIPSEV5a is provided in the Supplementary (Sect. 1.1) showing a high agreement for PM₁₀ (within few percent also at regional level) and less good agreement for the other aerosol components. Comparing global totals, we find 1% deviation for PM₁₀, 12% for PM_{2.5}, 17% for OC and 43% for BC (mainly due to the likely underestimation of the EDGAR v4.3.2 emissions compared to the ECLIPSEV5a of coal combustion in residential activities in China and India). Rather good agreement for the top emitting regions is found, while larger discrepancies are calculated for low emitting countries. Part of the discrepancies between ECLIPSEV5a and EDGAR v4.3.2 can be explained by not accounting for non-commercially sold fuels, such as diesel to run communication towers in India (Klimont et al., 2017) or coal and rubbish (Klimont et al., 2017; Bond et al., 2007), and wood, wood waste and pellets (Denier van der Gon et al., 2015). Because of the global coverage and the lack local information on super emitters (in particular super emitting vehicles, cold starts), the particulate emissions of EDGAR v4.3.2 are known to miss for some countries the 10% highly polluting activities with 10 times larger PM_{2.5} emission factor (Klimont et al., 2017 and references therein). The differences between the different EDGAR versions can be explained by data updates (e.g. activity data as discussed online for the difference between v4.2 and v4.1, EFs for SO₂, PM and NMVOC, the latter documented Huang et al. 2017), technologies and abatements). The two most recent EDGAR releases, v4.3.1 and v4.3.2, converge for almost all sources, except for the biofuel consumption in the residential sector for which the IEA activity data was known to have changed method (towards higher Tier) relying on comparable activity data. A significant update has also been made for the ferroalloys production sector, production of chemicals, production of fuels, residential sector and solid waste, mainly affecting CO emissions. The Lamarque et al. (2010) inventory shows a huge underestimation of NO_x



emissions **although we cannot fully understand** Finally, for EDGAR v4.3.2, a quality control procedure with full evaluation of the time series and gridmaps checking for gaps in the 1970-2102 time series or outliers and the closure of the particulate matter mass balance (e.g. $PM_{2.5} \leq PM_{10}$ and $BC+OC \leq PM_{2.5}$) have been performed. The closure of PM mass balance needs to be verified since each PM component is independently estimated from the others.

3.3 Regional air pollutant uncertainty analysis

Crippa et al. (2017) provide uncertainty estimates for gaseous and particulate matter emissions for all world regions based on the uncertainty estimates of the activity data and of the emission factors for each emission sector, pollutant and country (see Eq. 2):

$$\sigma(C, x, t) = \left(\sum_i \left(\sigma_{AD_i(C,t)}^2 + \sigma_{TECH_i(C,t)}^2 + \sigma_{EOP_i(C,t)}^2 + \sigma_{EF_i(C,x,t)}^2 + \sigma_{RED_i(C,x,t)}^2 \right) \left(\frac{EM_i(C, x, t)}{EM_{tot}(C, x, t)} \right)^2 \right)^{1/2} \quad (2)$$

with the standard deviations σ of the activity, technology, end-of-pipe data, emission factors and reduction factors for each pollutant x and country C .

Based on the assumption of lognormal distribution of the calculated uncertainties (Bond et al., 2004), we evaluated the upper and lower range of emission estimates multiplying and dividing the EDGAR v4.3.2 base emissions by $(1+\sigma_{p,c})$, respectively. Among all air pollutants (refer to Table S4), SO_2 has the smallest uncertainty at regional level (in 2012 variation between 14.4% and 47.6%); the uncertainty of NO_x varies in 2010 between 17.2% and 69.4% (with the exception of Brazil which reaches an uncertainty up to 123.5%), CO between 25.9% and 64.6% for industrialized countries (and up to 123.4% for emerging and developing economies) and $NM VOC$ between 32.7% and 73.6% for industrialized countries and above 100% (up to 147.5%) for non-Annex I countries and emerging economies. The uncertainty of NH_3 is the largest among all pollutants because of the high uncertainty both of agricultural statistics and emission factors (range of variation in 2012: 186% and 294.4%). **The aerosol emissions are in general characterized by rather high uncertainties** in a range of variation in 2012 between 57.4 and 109.1% for PM_{10} , between 49 and 91.4% for $PM_{2.5}$, between 46.8 and 92% for BC and between 88.7 and 153.2% for OC , consistently with the results of Bond et al (2004) reporting a factor of 2 for the uncertainty of the organic components. As discussed earlier, higher uncertainties in PM emissions might come from super emitting vehicles which are not considered in this study. Therefore, the error band range presented by Klimont et al. (2017) for these components is much wider than what we find in our work. due to the high uncertainty In general, the emission uncertainty is reducing over time for industrialized countries (e.g. SO_2 , CO , $PM_{2.5}$ for USA and EU28 and to a minor extent also NO_x), while the uncertainty band is larger for China and developing countries in particular due to the larger contribution of highly uncertain sector. We note that our uncertainty analysis using the relative values only estimate the uncertainty on the estimated part of the emissions and does not account for the missing superemitting part. In the case of PM our uncertainty band might be a factor 2 underestimated.



The uncertainty estimates shown in Fig. 6 as well as in Tables S4 and Fig. S1.4 are strongly determined by the relative contribution of each anthropogenic sector over time to the total emissions of a certain region, therefore we do not always observe a decreasing trend in the corresponding overall component uncertainty. For example, the uncertainty of NH₃ emissions in China (Fig. S1.4) is growing with a faster rate compared to the corresponding emissions, due to the very large uncertainty of the agricultural sector (use of fertilizers) and manure management whose contribution represented 69 % of total Chinese emissions in 1970 and 97% in 2012. Similarly, the uncertainty band of OC emissions in China (Fig. S1.4) shows a larger increase from 1985 to 1992 compared to the corresponding emissions due to the larger share of the residential combustion of biomass and coal emissions during those years which are very uncertain.

4 Emission metrics: implied emission factors, per capita and per GDP emissions

4.1 Evaluation of implied emission factors

Implied emission factors can be used as a metric of emission intensity of anthropogenic activities for each country and they have been calculated following the methodology by Janssens-Maenhout et al. (2015). Figure 7 shows the implied emission factors calculated for aggregated emission sectors (as defined in Sect. 2.1), namely “energy”, “industry”, “residential”, “transport” and “agriculture” from the EDGAR v4.3.2 database. Box plot statistics (10°, 25°, 50°, 75° and 90° percentiles) represent the variability amongst countries of the implied EFs in 2010 (2010 has been chosen for comparability with the HTAP_v2.2 inventory). The variability across countries is also investigated with the representation of the median implied EFs for low-income (LIC) and high-income (HIC) countries, showing for all pollutants and sectors much higher implied EFs for LIC than for HIC. The comparison with the corresponding implied EFs obtained for the HTAP_v2.2 emission data is also reported (refer to Janssens-Maenhout et al., 2015) showing rather good agreement with the exception of the industrial sector for most of the pollutants and the agricultural sector for NH₃ due to different emissions and activity data used for these two emission inventories. Table S1 of the Supplementary (Sect. 1.2) shows a detailed comparison of the implied emission factors of selected regions (EU28, USA, China, India, Russia and Japan) with the global median values for all pollutants and sectors.

The highest implied EFs for most of the pollutants emitted in the energy sector are found in developing regions, such as Africa, Latin America, Indonesia, India, but also Central Asia and Middle East, while lower values are observed for industrialized countries (USA, Europe, Japan), Korea and China. A different picture emerges for the industrial and transport sectors, where in addition to the aforementioned regions, also in China very high implied EFs are computed. On the contrary, the implied EFs for NH₃ related with the emissions of the transport sector are larger for USA, Oceania, Canada, Korea and Japan due to the deployment of gasoline vehicles equipped with NO_x reduction catalysts (producing N₂ and some other nitrogen components such as NH₃) and oxidize CO and unburned hydrocarbons (HC) to CO₂ and H₂O. The residential sector shows the smallest range of variation of the implied EFs for



most of the gaseous pollutants, due to the fact that less controls are applied both on the fuel used and combustion temperature (although industrialized countries have in general lower CO emission factors due to the deployment of burners with higher combustion efficiency). Despite of the low range in EFs, we should bear in mind that PM emission factors for the residential sector are the highest compared to all other activities, with the exception of some industrialized countries where the implementation of particulate filters on the stoves could have reduced significantly PM emissions.

For 1970-2012, the implied EFs were mostly decreasing. The implied EF for SO₂ for energy activities decreased on average by ca 60%, with a range of variation between 4 and 93% depending on the region. They ranged between 0.94 and 0.1 ton/TJ for OECD Europe, between 0.97 and 0.6 ton/TJ for Central Europe, between 1.1 and 0.25 ton/TJ for USA and between 1.03 and 0.23 ton/TJ for China. On the global average, NO_x implied EFs were decreasing from 1970 to 2012 with a smaller rate compared to SO₂ and by ca 30%. The residential sector is characterized by rather stable implied EFs (both for CO and the aerosol components), showing an average decrease of 30% for CO and 35% for PM_{2.5}. Africa, and other developing regions, show negligible variation in implied EFs over time due to the enhanced contribution of residential activities and higher emissions from biomass combustion. The implied EFs for the road transport sector were strongly decreasing for NO_x and CO in particular in industrialized countries from 1970 to 2012 with a global average decrease of 37% for NO_x and 67% for CO. The implied EFs for CO for the road transport sector varied over time from 7.7 to 1.7 ton/TJ for USA, from 8.8 to 0.4 ton/TJ for OECD Europe, from 7.2 to 0.9 ton/TJ for Central Europe and from 16 to 1.9 ton/TJ for China.

4.2 Evaluation of per capita and per GDP emissions for different groups of countries

In order to compare countries with differing degree of development and population, 2010 per capita emissions (Fig. 8) have been calculated for each pollutant and income level. The definition of country groups based on their income is consistent with the approach adopted by Janssens-Maenhout et al. (2015) and reported in Table S5. The comparison with the HTAP_v2.2 per capita emission estimates (Janssens-Maenhout et al., 2015) is also shown in Fig. 8 being the HTAP_v2.2 inventory based on official national inventory data. In addition, the emissions per income (or per GDP, corrected for the Purchasing Power Parity in 2010, IMF/WEO (2017)) are compared for the different pollutants in Fig. 9. Tables S2 and S3 of Sect. 1.3 of the Supplementary Information compare these values by macro region. HIC countries show the highest per capita emissions for most of the gaseous pollutants, representing the intensity of the anthropogenic activities associated with their industrial development. On the contrary particulate matter per capita emissions are higher for low and low middle compared to high income countries due to the lack of air pollution control equipment such as particulate filters and electrostatic precipitators together with the larger deployment of biomass based fuel, leading to high uncontrolled PM emissions mainly for household purposes. Among all air pollutants, CO shows the highest per GDP emissions and the largest variation over all countries reflecting the degree of economic activity in the world.



Similarly to the per capita emissions, industrialized countries have lower per GDP emissions of PM, while China, India and emerging/developing countries (Table S3) show the highest PM per GDP emissions due to the deployment of less clean technologies.

5 Ratios of co-emitted species

Combustion processes emit not only CO₂, but also a variety of other air pollutants, like NO_x, CO, SO₂ and PM. Depending on the fuel type, combustion technology and process, abatement measures, etc., source related emission ratios of co-emitted species are measured. In particular, very local combustion sources could alter the background concentrations of CO₂ and other pollutants and an analysis of the changes of the relative abundances of such pollutants could indicate and quantify the type of sources present in a certain area, when using the appropriate spatial resolution. Large scale events, such as fires can be distinguished using NO₂ and CO in addition to CO₂, as shown by Silva et al. (2017). These fire emissions are not included in our database. For smaller scale sources and point sources, high spatial resolution and plume modeling is needed to isolate the single sources, as shown by Nassar et al. (2017) in the case of a power plant. EDGAR does not have this high resolution, but the emission factors for the single multi-pollutant sources are available with the implied emission factors and the locations of the point sources for e.g. the energy sector is available in the sector-specific gridmap.

The EDGAR inventory provides estimates of co-emitted pollutants in addition to the greenhouse gases; however, as discussed in Sect. 3, even emissions from combustion processes are often poorly characterized in particular in developing regions due to scarce information on fuel consumed, deployed technologies and applied abatement measures. In order to better constrain emission inventories estimates, ground-based and satellite measurements can partly complement the information related with combustion emissions. For example, Silva et al. (2017) focus their study on satellite observations of CO₂, NO₂ and CO emitted by combustion sources and show that the analysis of co-emitted species could provide constraints on emission inventories, and be useful in monitoring trends and understanding regional-scale combustion processes. Due to the global coverage, historical time series and consistent emission estimates for both greenhouse gases and air pollutants and world countries, the EDGAR emissions of CO₂ and co-emitted pollutants could be coupled with the information retrieved by satellite measurements. The work by Streets et al. (2013) provide an overview on the current capabilities and limitations of satellite observations to measure air pollutant emissions such as SO₂, NO_x, CO, NMVOC, NH₃, PM, CH₄ and CO₂ as well as the methodology behind their emission estimation. Several other studies analyse satellite retrievals of emission ratios of co-emitted pollutants to identify multi-pollutant sources and possible proxies to estimate from e.g. CO₂ emissions the emissions of other compounds (Konovalov et al., 2016; Fioletov et al., 2017; Geng et al., 2017).

In this section, we analyse the emission ratios of co-emitted pollutants as provided by the EDGAR database (this calculation is not performed at gridcell level but considering the technology based emission factors and activities). These emission ratios are determined by the



type of fuel and the technology and as such differ by region (Fig. 10). Emission ratios of co-emitted species are strongly dependent on human activities and technologies in the emitting sector, which also change over time. In general we find lower emission ratios of each species to CO₂, as well as a smaller range of variation, in 2012 than in 1970 for most of the sectors (see also Fig. 11), because of a decoupling of air pollutant emissions from energy production due to global development towards clean air technologies. The global emission ratios of NO_x/CO₂ (and NO_x/CO) are the highest for the power generation sector, due to the high combustion temperatures producing high levels of NO_x and low CO, as shown in Fig. 11. The NO_x/CO₂ overall emission ratio in Mexico shows an increasing trend because of the corresponding increasing ratios of the transport and residential sectors (see Figs. 13 and 14). The CO/CO₂ emission ratio is the highest for the road transport and partly the residential sectors (both in 1970 and 2012) due to the low efficient combustion of vehicles and small scale combustion activities compared to power plants. The spike observed for Indonesia in 1990 is partly artificial and related with the contribution of industrial combustion activities, which were not estimated for earlier years. The SO₂/CO₂ emission ratio shows the largest decrease from 1970 to 2012 in particular affecting the power generation sector, due to the implementation of international conventions (e.g. CLRTAP) regulating acidifying gases and air quality together with regulations on the sulphur content of the fuels. The PM₁₀/CO₂ emission ratio is the largest for the residential sector due to the scarce implementation of abatement measures, lack of strict regulations, low quality fuels used for household purposes and often inefficient combustion processes.

The analysis of the power generation („Energy“) sector (Fig. S3a) for different countries reveals mainly decreasing trends for the NO_x/CO ratios but there is no generic trend for the ratio of CO, NO_x and SO₂ over CO₂. The largest reductions over time are computed for the SO₂/CO₂ ratios for developed countries, in particular those with a fuel shift from coal to gas, such as OECD-Europe but also USA and Russia. Decreases in NO_x/CO₂ ratios are present in many countries, OECD Europe, USA, Japan, Korea but also Mexico, Northern Africa, Southeastern Asia and China, reflecting the penetration of low-NO_x burners. NO_x/CO₂ and CO/CO₂ ratios are high and increasing till the year 2000 when they reach a plateau for least developed regions, such as Eastern Africa and Rest Central America. Our analysis of the transport sector (Fig. S3b) shows large differences between 1970 and 2012 due to a large penetration of clean air technologies, where the CO and NO_x emission factors have been decreasing considerably with the penetration of the vehicle emission standards, contrary to the CO₂ emission factor. The degree of regional development towards environmentally enhanced vehicles is directly reflected in the graphs of Fig. 13 showing a strong decrease for the CO/CO₂ ratio in developed regions, while China is showing an accelerated decrease since the 2000s. Even though the residential sector is not expected to show the same penetration of clean air technologies as the transport sector, large decreases of the CO/CO₂ ratios over time are generally calculated for almost all world regions. In particular SO₂/CO₂ ratios have decreased due to changes in the type of fuel used, most strongly in USA, Europe, Russia and Japan but also in China. However, contrary to CO/CO₂, the NO_x/CO₂ ratios did not show large improvements, which yielded also to the increases in NO_x/CO, as presented in Fig. S3c.



6 Gridded emissions

Gridded emissions represent an asset of the EDGAR database widely used by the scientific air quality and climate modeling communities. As mentioned in the introduction, in this section we do not analyze all the detailed information included within each gridmap (EDGAR comprises 42 years of gridmaps for 26 aggregated sectors and 9 substances), but rather try to inform the users about the type of information included in the gridded emissions and suggesting possible use of such data and analysis. In order to particularly address the satellite community, in the following we will focus on the emissions of the latest 5 years available in EDGAR v4.3.2 (2007-2012), investigating i) the possibility to use emission sector shares at gridcell level (Sect. 6.1) to retrieve from total column measurements the sector composition of the emissions and ii) the evolution of high emitting areas over time and space (hot spots evolution, Sect. 6.2). We selected a time period of 5 years because of detectable emissions trends and consistency of the EDGAR proxy data over that time frame.

6.1 Gridded emission sector shares

In the perspective of providing more insights on the composition of the total emissions and source decomposition within a single gridcell, the EDGAR v4.3.2 provides also the emission sector shares at gridcell level as NetCDF files at the http://edgar.jrc.ec.europa.eu/overview.php?v=432_AP&SECURE=123. Emission shares of each sector in total emissions are calculated for 2012 for each pollutant (NO_x, CO, SO₂, PM_{2.5}) and for CO₂ as reference proxy for activity (including both the fossil and biogenic components). This information can be used, e.g., for analysis of different sector emission shares for urban and rural locations, or for different countries, and to compare to the sector composition of total column measurements performed e.g. by satellites. However, it is important to mention that the assignment of sectorial information per gridcell and the calculation of emission ratios of co-emitted pollutants are subject to high uncertainty, including both the uncertainty about co-emission and the one related with the quality of the spatial allocation in the gridmaps. As the total emissions of the different pollutants show different trends over the past, it is expected that these sector shares change with time. The scatter plots shown in Fig. 12 show the trends of emission sector shares over the considered 5-year time step (2007-2012). In regions with relatively small trends, sector specific emission shares can be safely used also for other years. The 1:1 line indicates no change between the share of each specific sector and cell between the two years; in addition the $\pm 20\%$ deviation from the 1:1 line is reported. Deviations from the 1:1 line can be due to large change in the emissions of specific sectors and/or to a change in the proxy data used for the spatial distribution. It is worth to mention that ratios deviating from 1 can represent a real change in that sector share, but they can also reflect a change in the shares of the other sectors due to their complementarity. The comparison of the 2012 vs. the 2007 sector share pictures is needed to evaluate the stability of the 2012 emission sector shares we provide and the possible need of annual gridmaps to track changes in emission sector shares. As shown in Table 1, the



energy sector is the one varying most over 5 year time (from 3.7% to 7.5% of the points in the scatter plots of all pollutants vary more than 20% between 2007 and 2012), being affected by the change in the proxy data (location of point sources) provided by the CARMAv3.0 database (2012) between the considered two years (refer to S3.1 for details about the CARMA database). This result gives the indication that to have more accurate point source emission estimates (like the ones of the energy sector), annual spatial proxy data would be needed, in order to track all the changes happening in that sector (e.g. opening, closure or refitting of power plants, switch towards a different fuel, change of capacity, etc.). 0.5% of the CO₂ emission shares from the industrial sector vary more than 20% between 2007 and 2012, in particular changes occur in specific regions like Argentina, Indonesia, Iran, etc., 1.7% of the cells are outside the 20% deviation band for the residential sector, in particular affecting Kazakhstan, United Arab Emirates etc. This is due both to changes in population distribution and residential emission changes but also to decrease of the shares of the other sectors. The transport sector shows rather stable spatial shares between 2007 and 2012 (only 1% of cells out of almost 2 million of cells vary more than 20%). The agriculture sector shows specific patterns, with higher shares over Northern Africa (Algeria, Tunisia, etc.), Cameroon, Ethiopia, South Africa, Zambia, part of Middle East and Australia, while decreases in agricultural shares are mainly observed in the sub Saharan areas, Mongolia, Kazakhstan, and areas of Latin America.

The scatter plots represented in Fig. 12 show similar patterns as for CO₂ also for all other, in particular for the energy and industrial sectors. When a single country is characterized by a significant change between 2007 and 2012, this is represented by a curved line in the scatters (e.g. in the SO₂ industry scatter plot the lower curved line represents a change in Turkey, or the upper curve in the NO_x residential scatter reflects an increase in 2012 for Kazakhstan). Here, we do not aim at addressing all the changes of the sector shares observed at gridcell level representing anyway a minority of the analyzed points. However, we want to highlight that for some countries significant differences might happen even from one year to another for specific sectors, and so an annual reporting of their emissions should be recommended to track peculiar changes.

Maps in Figs. 13 and 14 represent the relative sector contribution of SO₂ and NO_x in 2012, while maps of Figs. S6 and S7 of the Supplementary Material are related to the sector shares of CO and PM_{2.5}. Considering SO₂ and NO_x emission shares, the energy sector is characterized by high emitting point sources in all world regions. On the other hand, the industrial sector is characterized by high emitting point sources over emerging economies and lower shares over USA and Europe, but also by flaring activities in the Northern Sea or around the Western coast of Africa. NO_x emitted by the transport sector is contributing for more than 50% over industrialized areas like USA, Europe and Australia, with 100% contribution over the sea due to the emissions of international shipping and aviation (this feature is common for all pollutants). The residential sector shows the largest shares over China, Africa and India (more than 50% relative contribution) for SO₂ (but also for CO and PM_{2.5} as shown in Figs. S6 and S7), while lower shares are observed for NO_x. The



agricultural sector is a dominant source in some areas of Northern Africa, Australia and mainly in Latin America (Argentina and Brazil).

6.2 Hot spots evolution over time

5 Figures 15a-c and S8a-b represent the ratio between 2012 and 2007 total emissions at gridcell
level for CO₂, NO_x, CO, SO₂ and PM_{2.5}. CO₂ is also shown as reference since it mainly
reflects changes in activity data. The green color represents a ratio between 0.8 and 1.2 (a
ratio of 1 represents no change between 2012 and 2007 emissions at gridcell level), the blue
10 colors refer to lower emissions in 2012 compared to 2007 while the yellow/red colors
represent higher emissions for the year 2012 compared to 2007. The colored bubbles represent
the top emitting 10000 gridcells at 0.1x0.1 degree over the whole globe for CO₂ and NO_x
in 2012 and in 2007, representing more than 94% of total CO₂ emissions (the same cells are then
used to produce the maps for all the other pollutants for comparability reasons), while their
size is proportional to the magnitude of the 2012 emission for the specific cell and pollutant,
15 therefore the radius of the bubbles cannot be directly compared among all the maps. For CO₂
(Fig. 15a) large areas of the world are covered by green colors, indicating no big changes
between the 2012 and 2007 emissions. Among all the green cells, the green bubbles represent
the top emitting cells in 2012 and/or 2007 which did not change significantly from 2007. The
very big yellow bubbles over China represent large high emitting sources which increased
20 their emissions from 2007 to 2012. On the other hand India is characterized by rather small,
but red bubbles, representing growing emitting points. NO_x and CO₂ maps are quite similar
(Figs.15a and 15b), meaning that coherent trends are observed for the two pollutants.
However, some differences can be observed over North America characterized by a
decreasing trend in NO_x emissions mainly from the transport sector counterbalanced by a
25 relatively stable fuel consumption (no significant trend is observed for CO₂ between 2007 and
2012).

SO₂ emissions (Fig. 15c) generally decreased from 2007 to 2012 in industrialized countries
(e.g. North America and Europe) mainly due to the deployment of lower sulphur content fuels
and technologies cleaning-up fuels cleaner (including deSO_x). However, some red hot spots
30 can be found in Central-Eastern Europe due to the larger deployment of low-grade coal and in
Mexico. Ship tracks along the American coasts and across the Atlantic Ocean are often red
representing increased shipping activity in this area (IEA reports the increase of diesel and
heavy residual oils as fuels in this sector by USA). Quite some hot spots are observed over the
Arabian Peninsula, Iraq, etc. due to the larger deployment of diesel and heavy residual fuel oil
35 for public electricity generation and the use of coal in the industrial sector.

CO and PM_{2.5} emission trends (refer to Figs. S8a-b) are mostly stable or decreasing over
industrialized regions because of the higher energy efficiency technologies. Strong decreases
are observed over Spain and Greece due to the economic recession, consistently with Fig.15a.
On the contrary, emerging economies like India and China are characterized by increasing
40 trend of CO and PM_{2.5} emissions.



7 Conclusion and outlook

This study builds on a previous study presented EDGAR v4.3.2 results for CO₂ and other GHGs (Janssens-Maenhout et al., 2017). In this work, we document the scientific global emission inventory EDGAR v4.3.2 to provide a consistently compiled and comprehensive dataset of anthropogenic emissions of gaseous and particulate air pollutants (SO₂, NO_x, CO, NMVOC, NH₃, PM₁₀, PM_{2.5}, BC, OC) over the time period 1970-2012 (with annual and monthly resolution) and spatially disaggregated gridmaps with 0.1°x0.1° resolution. A strength of EDGAR v4.3.2 is that the bottom-up emissions calculation methodology is consistently applied for all world countries, in a sectorial structure also used to compute greenhouse gases by IPCC, allowing consistent co-benefit analysis of GHG emission reduction strategies to air pollutants. In addition to the emission time series, we provide emissions per capita and per GDP, as well as implied EFs (emissions per unit of energy or product) to allow further analysis of efficiency and comparability between countries. We find that the calculated implied EFs are higher for low income compared to high-income countries, but overall they were decreasing from 1970 to 2012. In addition, we present emission ratios of co-emitted pollutants, in particular CO, NO_x and SO₂ to CO₂. We do hope that the combination of this emission information with atmospheric observations (in-site or spaceborne) can further improve our understanding of the emissions and the driving human activities. The analysis of emission hot spots using the gridded emissions identifies a growing amount of high-emitting areas (China, India, Middle East and some Southern American countries) in the world, with important implications for global air quality. In contrast, Europe or USA shows rather stable or decreasing emissions. To better constrain emission inventories' estimates with ground-based and satellite measurements we investigated the emission ratios of CO/CO₂, NO_x/CO₂, SO₂/CO₂ and PM/CO₂. Lower emission ratios of each species to CO₂ are found in 2012 than in 1970 for most of the sectors due to global development towards clean air technologies, in particular the SO₂/CO₂ emission ratio shows the largest decrease from 1970 to 2012. We also investigate the sector-specific emission ratios of each pollutant to CO₂. The NO_x/CO₂ ratios are the highest for the power generation sector, due to the high combustion temperatures producing high levels of NO_x and low CO, while the PM₁₀/CO₂ emission ratio is the largest for the residential sector due to the scarce implementation of abatement measures, lack of strict regulations, low quality fuels used for household purposes and often inefficient combustion processes. Finally, the assessment of the stability of sector-specific emission shares at grid-cell level over time aims at providing insights to the modelling and satellite communities on the sector disaggregated gridded emissions to be applied at bulk composition of the atmosphere.

8 Access to the data

Annual grid-maps for all gaseous and particulate air pollutants and sectors covering the years 1970-2012 are available as txt (expressed in the unit: ton substance per gridcell) and NetCDF (expressed in kg substance/m²/s) with 0.1°x0.1° spatial resolution in the map gallery at http://edgar.jrc.ec.europa.eu/overview.php?v=432_AP&SECURE=123. Data are presented



online for each source category with annual and monthly global emission gridmaps with 0.1°x0.1° resolution and are registered under DOI: https://data.europa.eu/doi/10.2904/JRC_DATASET_EDGAR and can be freely accessed via the EDGAR website http://edgar.jrc.ec.europa.eu/overview.php?v=432_AP&SECURE=123.

- 5 In addition, monthly air pollutant grid-maps are produced for 2012 and are available per sector and substance. The DOI associated with the EDGAR v4.3.2 air pollutant release DOI: https://data.europa.eu/doi/10.2904/JRC_DATASET_EDGAR.

9 Acknowledgement

- 10 The EDGAR database compilation was initiated by J. Olivier (PBL), but after 2008 under the overall responsibility of the Joint Research Centre. Over the years a number of scientists and technicians have supported the EDGAR- we are grateful for their contributions. Specifically, the EDGARv4 development profited from the substantial contribution of the authors John A. van Aardenne, Suvi Monni, Ulrike Doering and Valerio Pagliari, when they were affiliated to JRC. The authors are further grateful to the IEA, K. Treanton and R. Quadrelli, for the
- 15 collaboration and data exchange of the energy related statistics, and to J. Wilson (JRC) for the thorough review and English proofreading.



References

- Anenberg, S. C., Schwartz, J., Vignati, E., Emberson, L., Muller, N. Z., West, J. J., Williams, M., Demkine, V., Hicks, W. K., and Kuylenstierna, J.: Global air quality and health co-benefits of mitigating near-term climate change through methane and black carbon emission controls, 2012.
- Bond, T. C., Streets, D. G., Yarber, K. F., Nelson, S. M., Woo, J.-H., and Klimont, Z.: A technology-based global inventory of black and organic carbon emissions from combustion, *Journal of Geophysical Research: Atmospheres*, 109, D14203, [10.1029/2003jd003697](https://doi.org/10.1029/2003jd003697), 2004.
- Bond, T. C., Bhardwaj, E., Dong, R., Jogani, R., Jung, S., Roden, C., Streets, D. G., and Trautmann, N. M.: Historical emissions of black and organic carbon aerosol from energy-related combustion, 1850–2000, *Global Biogeochemical Cycles*, 21, GB2018, [10.1029/2006gb002840](https://doi.org/10.1029/2006gb002840), 2007.
- CARMAv3.0: Carbon Monitoring for Action: power plants: data, version v3.0 <http://carma.org/plant>, 2012.
- Crippa, M., Janssens-Maenhout, G., Dentener, F., Guizzardi, D., Sindelarova, K., Muntean, M., Van Dingenen, R., Granier, C.: Forty years of improvements in European air quality: the role of EU policy–industry interplay, *Atmos. Chem. Phys.*, 16, 3825–3841, 2016, doi:10.5194/acp-16-3825-2016, 2016a.
- Crippa, M., Janssens-Maenhout, G., Guizzardi, D., and Galmarini, S.: EU Effect: Exporting Emission Regulations through Global Market Economy, *Journal of Environmental Management*, 183, 959–971, <http://dx.doi.org/10.1016/j.jenvman.2016.09.068>, 2016b.
- Crippa, M., Janssens-Maenhout, G., Guizzardi, D., Van Dingenen, R., and Dentener, F.: Sectorial and regional uncertainty analysis of the contribution of anthropogenic emissions to regional and global PM_{2.5} health impacts, *Atmos. Chem. Phys. Discuss.*, <https://doi.org/10.5194/acp-2017-779>, in review, 2017.
- Dalsøren, S. B., Eide, M. S., Endresen, Ø., Mjelde, A., Gravir, G., and Isaksen, I. S. A.: Update on emissions and environmental impacts from the international fleet of ships: the contribution from major ship types and ports, *Atmos. Chem. Phys.*, 9, 2171–2194, [10.5194/acp-9-2171-2009](https://doi.org/10.5194/acp-9-2171-2009), 2009.
- Denier Van Der Gon, H., Bergström, R., Fountoukis, C., Johansson, C., Pandis, S., Simpson, D., and Visschedijk, A.: Particulate emissions from residential wood combustion in Europe—revised estimates and an evaluation, *Atmospheric Chemistry and Physics*, 15, 6503–6519, 2015.
- EC-JRC/PBL, European Commission, Joint Research Centre (JRC)/Netherlands Environmental Assessment Agency (PBL): Emission Database for Global Atmospheric Research (EDGAR), release EDGAR version 4.2. <http://edgar.jrc.ec.europa.eu/overview.php?v=42>, 2011.
- EMEP/EEA, Emission Inventory guidebook, European Environment Agency. <https://www.eea.europa.eu/publications/emep-eea-guidebook-2013>, 2013.



- EMEP/EEA: EMEP/EEA air pollutant emission inventory guidebook 2016, European Environment Agency, Copenhagen, 2016.
- EPRT: European Pollutant Transfer Register, database version v4.2, <http://prtr.ec.europa.eu/>, 2012.
- 5 EU Regulation No 377/2014 of the European Parliament and of the Council of 3 April 2014 establishing the Copernicus Programme and repealing Regulation (EU) No. 911/2010, <http://eur-lex.europa.eu/legal-content/EN/TXT/PDF/?uri=CELEX:32014R0377&qid=1508755044639&from=EN>
- 10 Eysers, C. J., Addleton, D., Atkinson, K., Broomhead, M. J., Christou, R. A., Elliff, T. E., Falk, R., Gee, I. L., Lee, D. S., Marizy, C., Michot, S., Middel, J., Newton, P., Norman, P., Plohr, M., Raper, D. W., and Stanciou, N.: AERO2k Global Aviation Emissions Inventories for 2002 and 2025, QinetiQ Ltd, Farnborough, Hampshire QINETIQ/04/01113, 2005.
- FAOSTAT: Statistics Division of the Food Agricultural Organisation (FAO). Live animal numbers, crop production, total nitrogen fertiliser consumption statistics till 2012, 2014.
- 15 <http://www.fao.org/faostat/en/#data/QD>, info retrieved 10.2016, 2016a.
- FAO: Forestry production and trade, pulpwood. <http://www.fao.org/faostat/en/#data/FO>, info retrieved 10.2016, 2016b.
- Fioletov, V., McLinden, C. A., Kharol, S. K., Krotkov, N. A., Li, C., Joiner, J., Moran, M. D., Vet, R., Visschedijk, A. J. H., and Denier van der Gon, H. A. C.: Multi-source SO₂ emission retrievals and consistency of satellite and surface measurements with reported emissions, *Atmos. Chem. Phys.*, 17, 12597-12616, 10.5194/acp-17-12597-2017, 2017.
- 20 Flemming, J., Benedetti, A., Inness, A., Engelen, R. J., Jones, L., Huijnen, V., Remy, S., Parrington, M., Suttie, M., Bozzo, A., Peuch, V.-H., Akritidis, D., and Katragkou, E.: The CAMS interim Reanalysis of Carbon Monoxide, Ozone and Aerosol for 2003–2015, *Atmos. Chem. Phys.*, 17, 1945-1983, <https://doi.org/10.5194/acp-17-1945-2017>, 2017.
- 25 Geng, G., Zhang, Q., Martin, R. V., Lin, J., Huo, H., Zheng, B., Wang, S., and He, K.: Impact of spatial proxies on the representation of bottom-up emission inventories: A satellite-based analysis, *Atmos. Chem. Phys.*, 17, 4131-4145, 10.5194/acp-17-4131-2017, 2017.
- Granier, C., Bessagnet, B., Bond, T., D'Angiola, A., Denier van der Gon, H., Frost, G., Heil, A., Kaiser, J., Kinne, S., Klimont, Z., Kloster, S., Lamarque, J.-F., Liousse, C., Masui, T., Meleux, F., Mieville, A., Ohara, T., Raut, J.-C., Riahi, K., Schultz, M., Smith, S., Thompson, A., Aardenne, J., Werf, G., and Vuuren, D.: Evolution of anthropogenic and biomass burning emissions of air pollutants at global and regional scales during the 1980–2010 period, *Climatic Change*, 109, 163-190, 10.1007/s10584-011-0154-1, 2011.
- 35 Hoesly, R. M., Smith, S. J., Feng, L., Klimont, Z., Janssens-Maenhout, G., Pitkanen, T., Seibert, J. J., Vu, L., Andres, R. J., Bolt, R. M., Bond, T. C., Dawidowski, L., Kholod, N., Kurokawa, J. I., Li, M., Liu, L., Lu, Z., Moura, M. C. P., O'Rourke, P. R., and Zhang, Q.: Historical (1750–2014) anthropogenic emissions of reactive gases and aerosols from the



- Community Emission Data System (CEDs), *Geosci. Model Dev. Discuss.*, 2017, 1-41, [10.5194/gmd-2017-43](https://doi.org/10.5194/gmd-2017-43), 2017.
- HTAP, UNECE: Hemispheric Transport of Air Pollution 2010: Part A: Ozone and Particulate Matter, *Air Pollution Studies No. 17*, edited by: Dentener, F., Keating, T., and Akimoto, H., ECE/EN.Air/100, ISSN 1014-4625, ISBN 978-92-1-117043-6, 2010.
- 5 Huang, G., Brook, R., Crippa, M., Janssens-Maenhout, G., Schieberle, C., Dore, C., Guizzardi, D., Muntean, M., Schaaf, E., Friedrich, R.: Speciation of anthropogenic emissions of non-methane volatile organic compounds: a global gridded data set for 1970-2012, *Atmos. Chem. Phys.*, doi:10.5194/acp-2017-65, 2017.
- 10 IEA: Energy Statistics of OECD and Non-OECD Countries. On-line data service. <http://data.iea.org>, 2014, 2017.
- IMF/WEO: World Economic Outlook Update January 2017, International Monetary Fund, 2017.
- Inness, A., Baier, F., Benedetti, A., Bouarar, I., Chabrillat, S., Clark, H., Clerbaux, C., 15 Coheur, P., Engelen, R. J., Errera, Q., Flemming, J., George, M., Granier, C., Hadji-Lazaro, J., Huijnen, V., Hurtmans, D., Jones, L., Kaiser, J. W., Kapsomenakis, J., Lefever, K., Leitão, J., Razinger, M., Richter, A., Schultz, M. G., Simmons, A. J., Suttie, M., Stein, O., Thépaut, J.-N., Thouret, V., Vrekoussis, M., Zerefos, C., and the MACC team: The MACC reanalysis: an 8 yr data set of atmospheric composition, *Atmos. Chem. Phys.*, 13, 4073-4109, 20 https://doi.org/10.5194/acp-13-4073-2013, 2013.
- IPCC: Revised 1996 IPCC Guidelines for National Greenhouse Gas Inventories IPCC/OECD/IEA, Paris, 1996.
- IPCC: Good Practice Guidance and Uncertainty Management in National Greenhouse Gas Inventories, IPCC-TSU NGGIP, Japan, 2000.
- 25 IPCC: 2006 IPCC Guidelines for National Greenhouse Gas Inventories. Eggleston, S., Buendia, L., Miwa, K., Ngara, T., Tanabe, K. (eds.). IPCC-TSU NGGIP, IGES, Hayama, Japan. www.ipcc-nggip.iges.or.jp/public/2006gl/index.html, 2006.
- IPCC: Intergovernmental Panel on Climate Change, Fifth Assessment Report, available at: <http://www.ipcc.ch/> 2013.
- 30 Janssens-Maenhout, G., Crippa, M., Guizzardi, D., Muntean, M., Schaaf, E., Dentener, F., Bergamaschi, P., Pagliari, V., Olivier, J. G. J., Peters, J. A. H. W., van Aardenne, J. A., Monni, S., Doering, U., and Petrescu, A. M. R.: EDGAR v4.3.2 Global Atlas of the three major Greenhouse Gas Emissions for the period 1970–2012, *Earth Syst. Sci. Data Discuss.*, <https://doi.org/10.5194/essd-2017-79>, in review, 2017.
- 35 Janssens-Maenhout, G., Crippa, M., Guizzardi, D., Dentener, F., Muntean, M., Pouliot, G., Keating, T., Zhang, Q., Kurokawa, J., Wankmüller, R., Denier van der Gon, H., Kuenen, J. J. P., Klimont, Z., Frost, G., Darras, S., Koffi, B., and Li, M.: HTAP_v2.2: a mosaic of regional and global emission grid maps for 2008 and 2010 to study hemispheric transport of air pollution, *Atmos. Chem. Phys.*, 15, 11411-11432, doi:10.5194/acp-15-11411-2015, 2015.



- Klimont, Z., Kupiainen, K., Heyes, C., Purohit, P., Cofala, J., Rafaj, P., Borken-Kleefeld, J., and Schöpp, W.: Global anthropogenic emissions of particulate matter including black carbon, *Atmos. Chem. Phys.*, 17, 8681-8723, 10.5194/acp-17-8681-2017, 2017.
- 5 Kononov, I. B., Berezin, E. V., Ciais, P., Broquet, G., Zhuravlev, R. V., and Janssens-Maenhout, G.: Estimation of fossil-fuel CO₂ emissions using satellite measurements of “proxy” species, *Atmos. Chem. Phys.*, 16, 13509-13540, 10.5194/acp-16-13509-2016, 2016.
- Lamarque, J.-F., Bond, T. C., Eyring, V., Granier, C., Heil, A., Klimont, Z., Lee, D., Liousse, C., Mieville, A., Owen, B., Schultz, M. G., Shindell, D., Smith, S. J., Stehfest, E., Van Aardenne, J., Cooper, O. R., Kainuma, M., Mahowald, N., McConnell, J. R., Naik, V., Riahi, K., and van Vuuren, D. P.: Historical (1850–2000) gridded anthropogenic and biomass burning emissions of reactive gases and aerosols: methodology and application, *Atmos. Chem. Phys.*, 10, 7017-7039, doi:10.5194/acp-10-7017-2010, 2010.
- 10 Maas, R., and Grennfelt, P.: Towards Cleaner Air. Scientific Assessment Report 2016, EMEP Steering Body and Working Group on Effects of the Convention on Long-Range Transboundary Air Pollution, Oslo., 2016.
- 15 Monks, P. S., Granier, C., Fuzzi, S., Stohl, A., Williams, M. L., Akimoto, H., Amann, M., Baklanov, A., Baltensperger, U., Bey, I., Blake, N., Blake, R. S., Carslaw, K., Cooper, O. R., Dentener, F., Fowler, D., Fragkou, E., Frost, G. J., Generoso, S., Ginoux, P., Grewe, V., Guenther, A., Hansson, H. C., Henne, S., Hjorth, J., Hofzumahaus, A., Huntrieser, H., Isaksen, I. S. A., Jenkin, M. E., Kaiser, J., Kanakidou, M., Klimont, Z., Kulmala, M., Laj, P., Lawrence, M. G., Lee, J. D., Liousse, C., Maione, M., McFiggans, G., Metzger, A., Mieville, A., Moussiopoulos, N., Orlando, J. J., O'Dowd, C. D., Palmer, P. I., Parrish, D. D., Petzold, A., Platt, U., Pöschl, U., Prévôt, A. S. H., Reeves, C. E., Reimann, S., Rudich, Y., Sellegri, K., Steinbrecher, R., Simpson, D., ten Brink, H., Theloke, J., van der Werf, G. R., Vautard, R., Vestreng, V., Vlachokostas, C., and von Glasow, R.: Atmospheric composition change – global and regional air quality, *Atmospheric Environment*, 43, 5268-5350, <http://dx.doi.org/10.1016/j.atmosenv.2009.08.021>, 2009.
- 25 Muntean, M., Janssens-Maenhout, G., Song, Giang, A., Selin, N.; Zhong, H., Zhao, Y., Olivier, J., Guizzardi, D., Crippa, M., Schaaf, E., Dentener, F.: Evaluating EDGARv4.tox2 speciated mercury emissions ex-post scenarios and their impacts on modelled global and regional wet deposition patterns, *Atmos. Env.*, submitted, 2018.
- 30 Nassar, R., Hill, T. G., McLinden, C. A., Wunch, D., Jones, D. B. A., and Crisp, D.: Quantifying CO₂ Emissions From Individual Power Plants From Space, *Geophysical Research Letters*, 44, 10,045-010,053, 10.1002/2017gl074702, 2017.
- 35 Reuter, M., Buchwitz, M., Hilboll, A., Richter, A., Schneising, O., Hilker, M., Heymann, J., Bovensmann, H., and Burrows, J.: Decreasing emissions of NO_x relative to CO₂ in East Asia inferred from satellite observations, *Nature Geoscience*, 7, 792-795, 2014.
- Seinfeld, J. H., and Pandis, S. N.: *Atmospheric Chemistry and Physics: From Air Pollution to Climate Change*, 2nd ed., John Wiley & Sons, Inc., New York, 2006.



- Silva, S., and Arellano, A.: Characterizing Regional-Scale Combustion Using Satellite Retrievals of CO, NO₂ and CO₂, *Remote Sensing*, 9, 744, 2017.
- Streets, D. G., Canty, T., Carmichael, G. R., de Foy, B., Dickerson, R. R., Duncan, B. N., Edwards, D. P., Haynes, J. A., Henze, D. K., Houyoux, M. R., Jacob, D. J., Krotkov, N. A., Lamsal, L. N., Liu, Y., Lu, Z., Martin, R. V., Pfister, G. G., Pinder, R. W., Salawitch, R. J., and Wecht, K. J.: Emissions estimation from satellite retrievals: A review of current capability, *Atmospheric Environment*, 77, 1011-1042, <https://doi.org/10.1016/j.atmosenv.2013.05.051>, 2013.
- UNFCCC, National Inventory Report, submissions of the greenhouse gas inventories for Annex I countries. http://unfccc.int/national_reports/annex_i_ghg_inventories/national_inventories_submissions/items/7383.php, 2014.
- UN STATS: Industrial Commodity Production Statistics 1970-2013, UN Statistics Division, <http://unstats.un.org/unsd/industry/publications.asp>, 2014.
- USGS: US Geological Survey Minerals Yearbook, US Geological Survey, Reston, Virginia, <http://mnminerals.usgs.gov/minerals/pubs/commodity>, 2014.
- US EPA: Global Anthropogenic Air Pollutant Emissions: 1990-2030, EPA report, 2014.
- Van Dingenen, R., Dentener, F. J., Raes, F., Krol, M. C., Emberson, L., and Cofala, J.: The global impact of ozone on agricultural crop yields under current and future air quality legislation, *Atmospheric Environment*, 43, 604-618, <http://dx.doi.org/10.1016/j.atmosenv.2008.10.033>, 2009.
- Wang, K. C., R. E. Dickinson, L. Su, and K. E. Trenberth, 2012: Contrasting trends of mass and optical properties of aerosols over the Northern Hemisphere from 1992 to 2011. *Atmos. Chem. Phys.*, 12, 9387-9398.
- WHO: Ambient air pollution: a global assessment of exposure and burden of disease, Geneva: World Health Organization, 2016.
- Zhao, Y., Nielsen, C. P., McElroy, M. B., Zhang, L., and Zhang, J.: CO emissions in China: Uncertainties and implications of improved energy efficiency and emission control, *Atmospheric Environment*, 49, 103-113, <https://doi.org/10.1016/j.atmosenv.2011.12.015>, 2012.



Tables

Table 1 – Fraction of gridcells (represented by each point) outside the 20% deviation band is reported together with the total number of emitting gridcells (in brackets).

	Fraction of points outside the 20% deviation band (total number of points)				
	ENERGY	INDUSTRY	TRANSPORT	RESIDENTIAL	AGRICULTURE
CO₂	5.9%(1.49E+4)	0.5% (1.45E+6)	1.0% (1.97E+6)	1.7% (1.44E+6)	0.8% (8.50E+5)
SO₂	7.5% (1.49E+4)	2.8% (1.34E+5)	1.9% (1.97E+6)	3.2% (1.44E+6)	1.3% (6.39E+5)
NO_x	6.4% (1.49E+4)	1.4% (1.25E+5)	0.4% (1.97E+6)	0.9% (1.44E+6)	0.6% (1.47E+6)
CO	3.7% (1.49E+4)	0.9% (1.25E+5)	2.0% (1.97E+6)	3.9% (1.44E+6)	2.0% (6.39E+5)
PM_{2.5}	4.5% (1.49E+4)	0.9% (1.39E+5)	1.1% (1.97E+6)	3.9% (1.44E+6)	3.8% (1.47E+6)

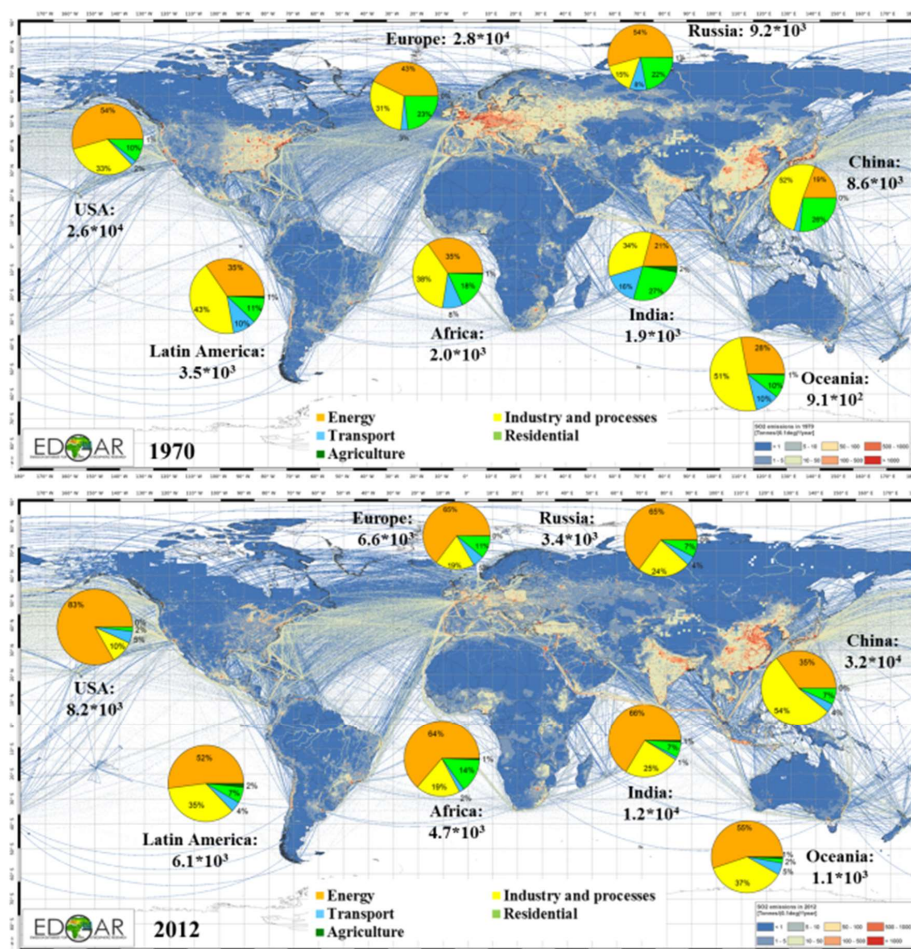
10

15

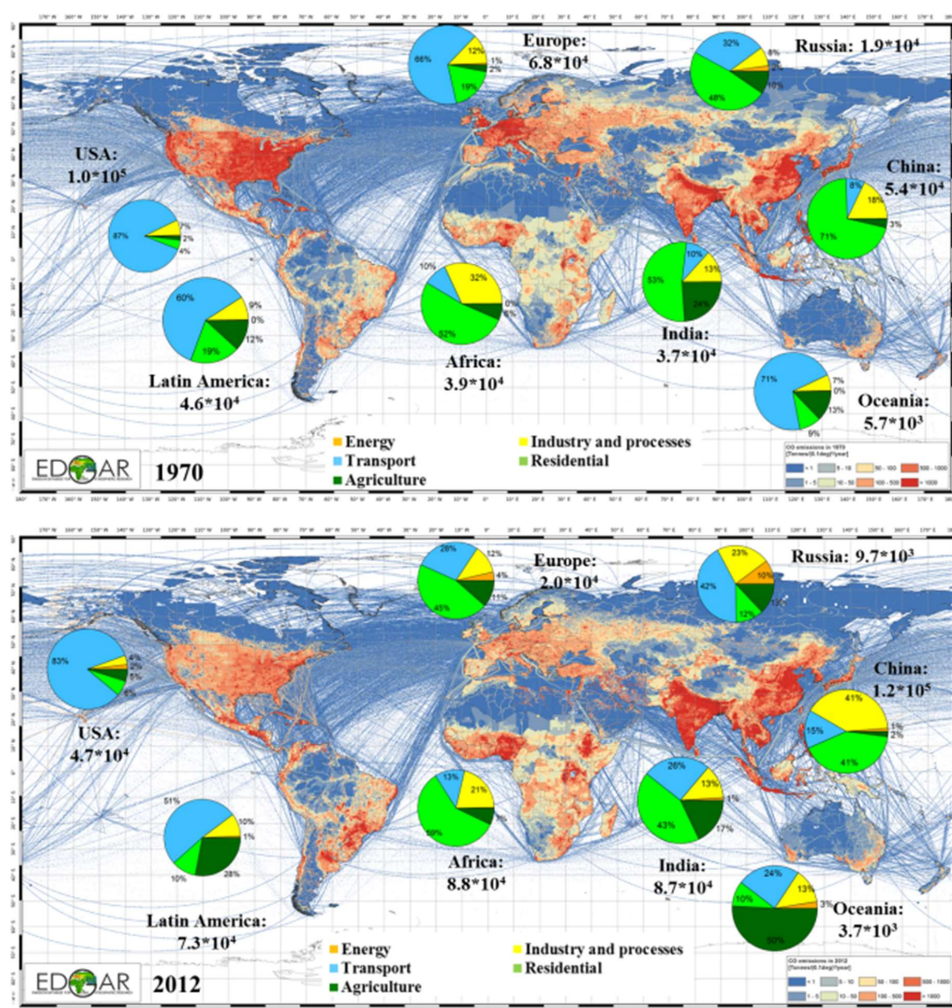
20



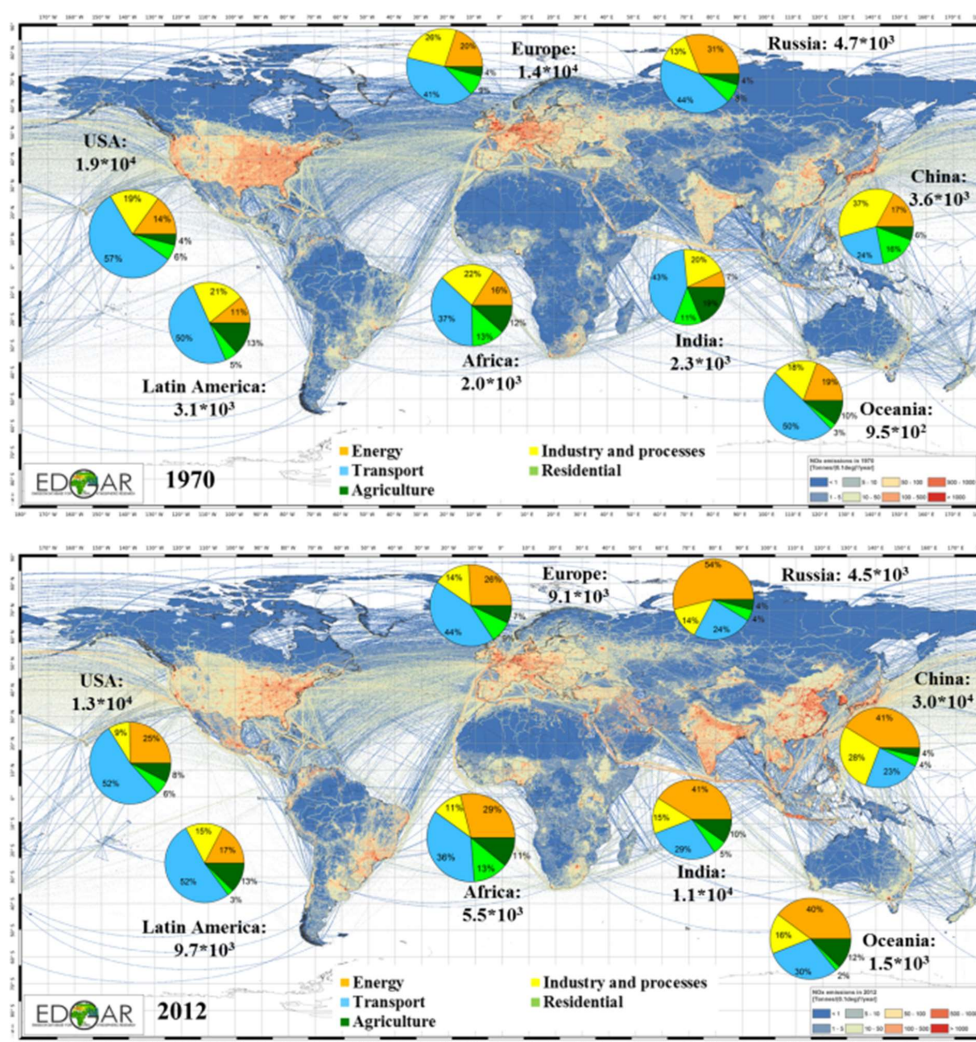
Figures



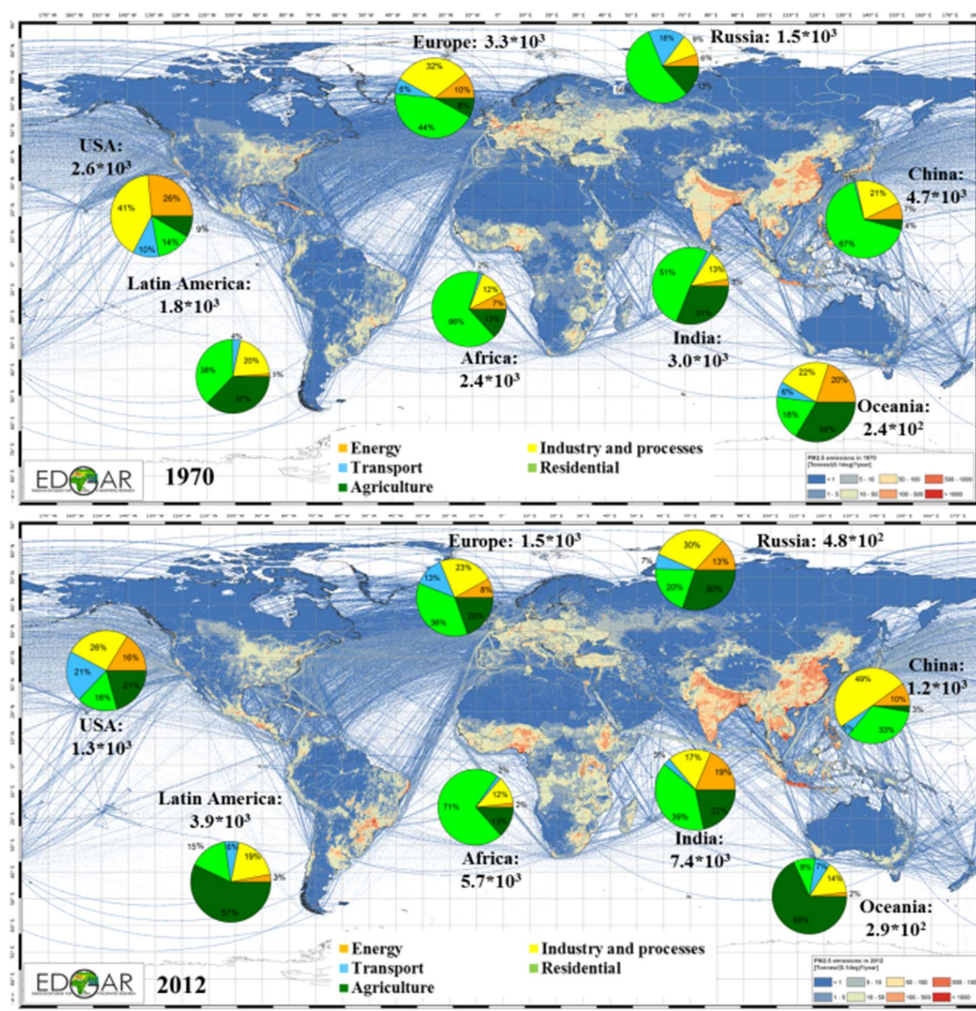
5 Figure 1 – SO₂ emission gridmaps and relative contribution of aggregated EDGAR sectors (Energy, Industry and processes, Transport, Residential and Agriculture) in world regions (pie charts) for 1970 and 2012. Total emissions (in kton/year) by region are also reported on top of each pie chart.



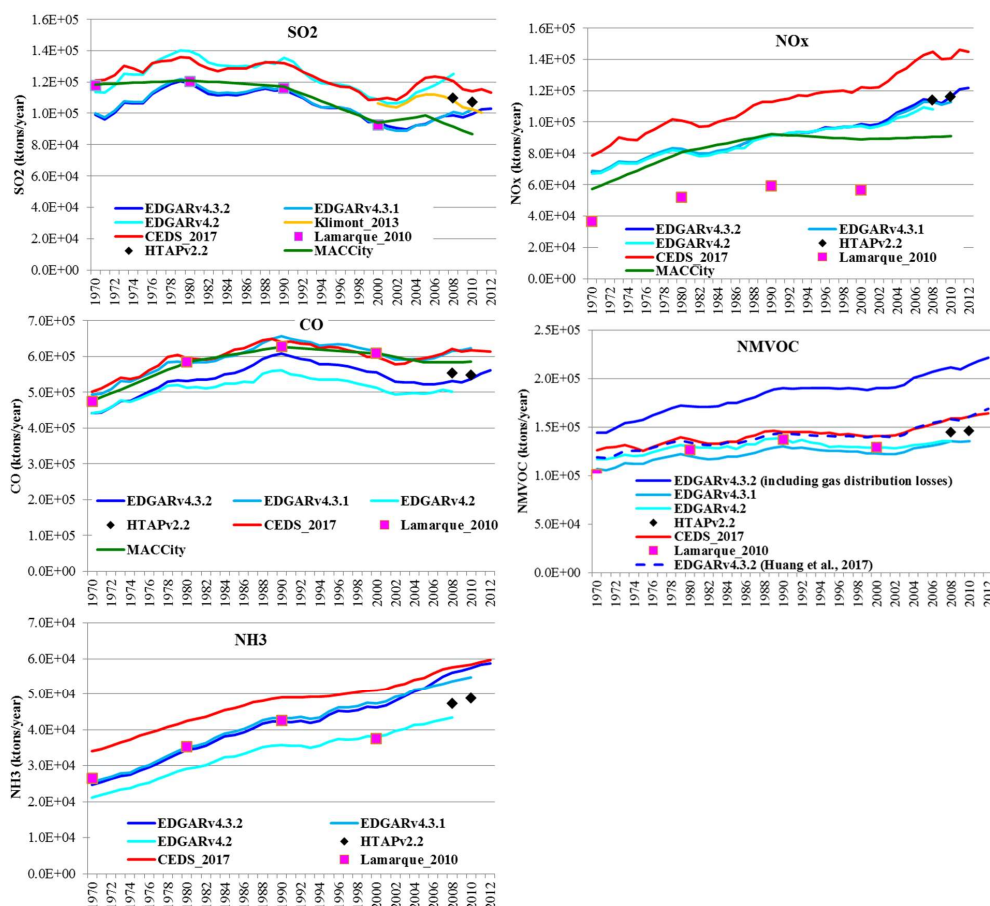
5 **Figure 2 – CO emission gridmaps and relative contribution of aggregated EDGAR sectors (Energy, Industry and processes, Transport, Residential and Agriculture) in world regions (pie charts) for 1970 and 2012. Total emissions (in kton/year) by region are also reported on top of each pie chart.**



5 Figure 3 – NOx emission gridmaps and relative contribution of aggregated EDGAR sectors (Energy, Industry and processes, Transport, Residential and Agriculture) in world regions (pie charts) for 1970 and 2012. Total emissions (in kton/year) by region are also reported on top of each pie chart.



5 **Figure 4 – PM_{2.5} emission gridmaps and relative contribution of aggregated EDGAR sectors (Energy, Industry and processes, Transport, Residential and Agriculture) in world regions (pie charts) for 1970 and 2012. Total emissions (in kton/year) by region are also reported on top of each pie chart.**



5 **Figure 5a – Comparison of global emission time series (1970-2012) of gaseous pollutants provided by different global emission inventories. The NMVOC graph presents two estimates for the EDGAR v4.3.2 database, one referring to the work of Huang et al. (2017) and the second one related with this study which also includes the emissions from the gas distribution losses.**

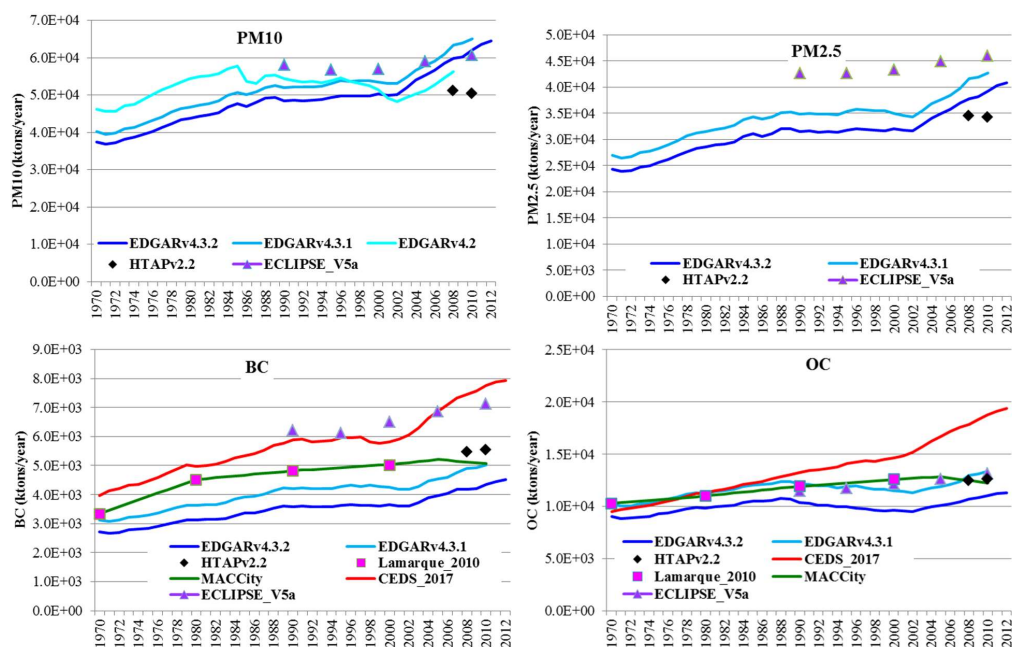
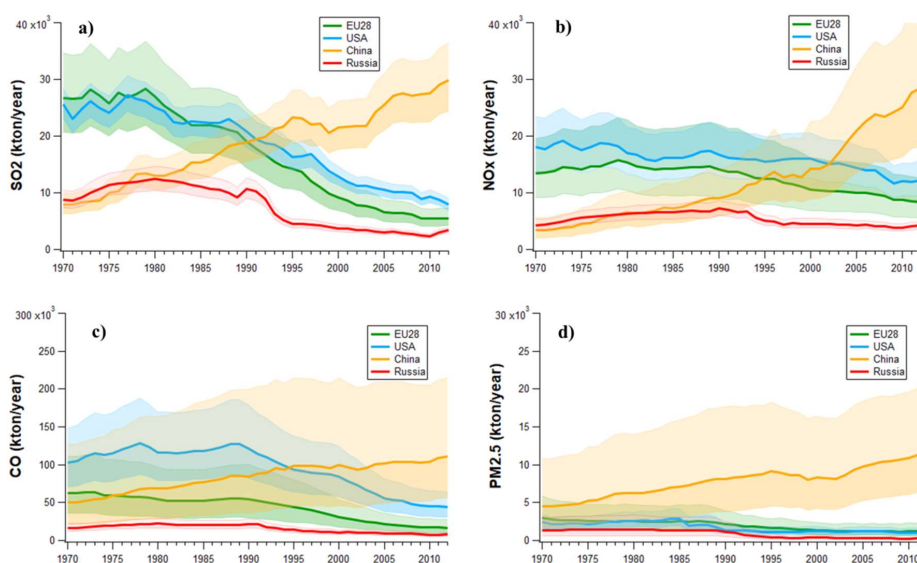
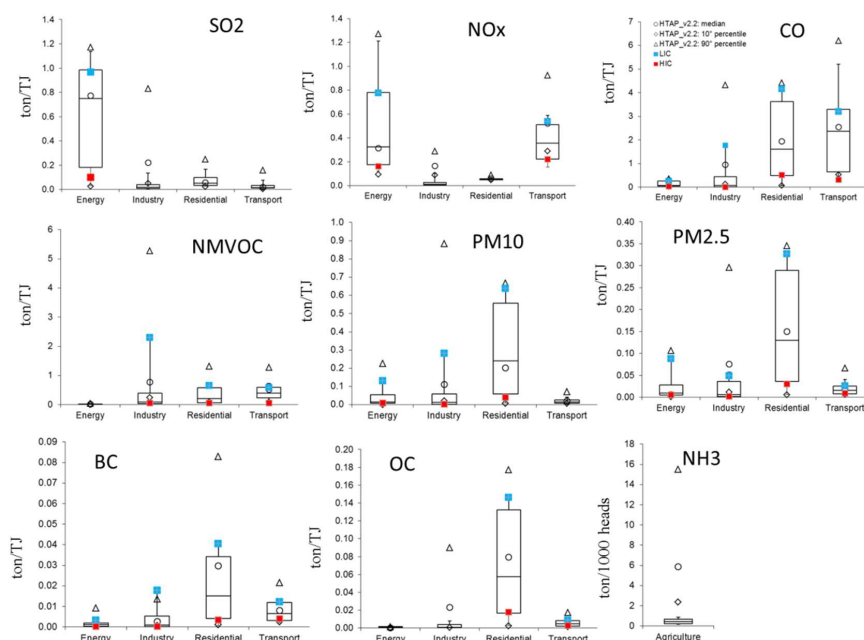


Figure 5b – Comparison of global emission time series (1970-2012) of aerosols provided by different global emission inventories. OC and BC are expressed in kton C/year.



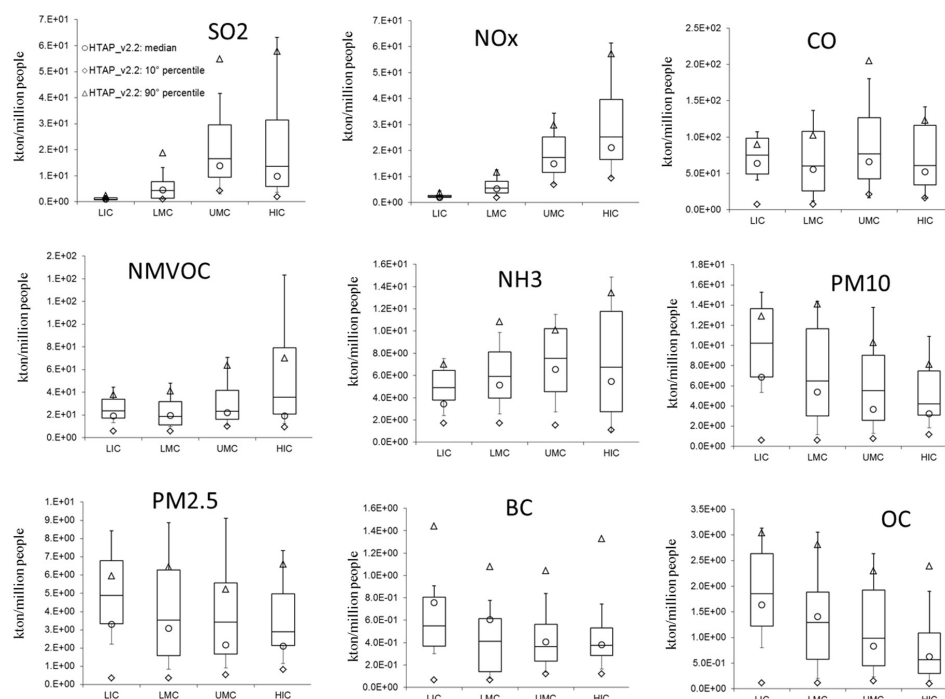
5

Figure 6 – Emission time series of SO₂, NO_x, CO and PM_{2.5} with uncertainty bands for top emitting countries/regions (China, USA, Russia and EU28).

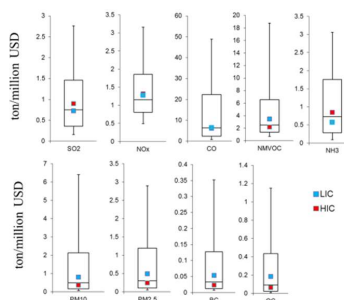


5 **Figure 7 - Implied emission factors calculated for 226 countries for aggregated emission**
 sectors “energy”, “industry”, “residential”, “transport” and “agriculture” from the
 EDGAR v4.3.2 database. Box plot statistics (10°, 25°, 50°, 75° and 90° percentiles)
 represent the country variability of the implied EFs in 2010. The comparison with
 the corresponding implied EFs obtained for the HTAP_v2.2 (Janssens-Maenhout et al.,
 2015) emission data, which excludes agricultural waste burning and field burning, is also
 10 reported. In addition, we report the median of low income and high-income countries
 (with light blue and red markers, respectively) for the sectors showing the larger
 variability across countries. Table S1 of the supplementary material reports implied EFs
 for all pollutants and sectors for selected regions differing for income level and the
 comparison with the global average.

15



5 **Figure 8 - Per capita air pollutant emissions in 2010 (for comparability with the HTAP_v2.2 inventory) per substance and group of countries are represented as box plots (10°, 25°, 50°, 75° and 90° percentiles): low income (LIC), lower middle income (LMC), upper middle income (UMC) and high income (HIC). The comparison with the HTAP_v2.2 estimates (circle=median, diamond=10° percentile, triangle=90° percentile) (refer to Janssens-Maenhout et al., 2015) is also reported.**



10 **Figure 9 - Pollutant specific emissions divided by GDP (g/USD) for the year 2010. Percentiles of emissions/GDP are reported in the box plots (10°, 25°, 50°, 75° and 90°), while the median of low income and high income countries is represented with light blue and red markers, respectively.**

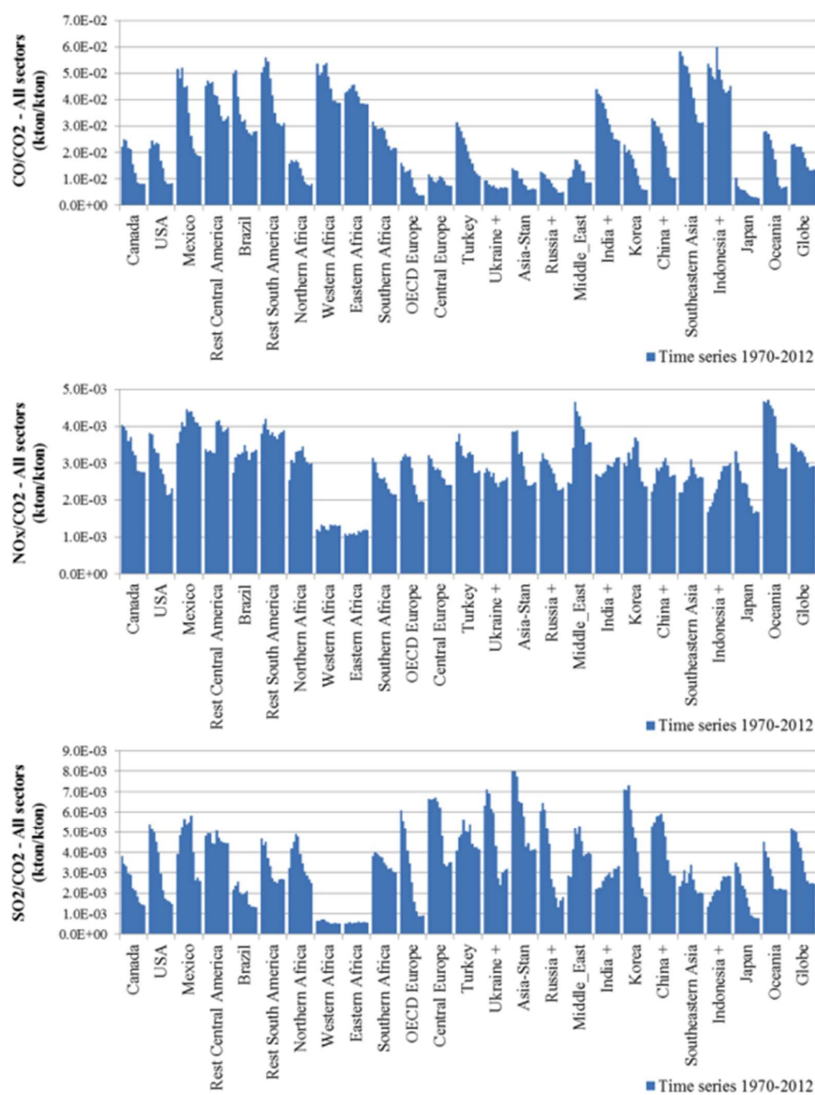
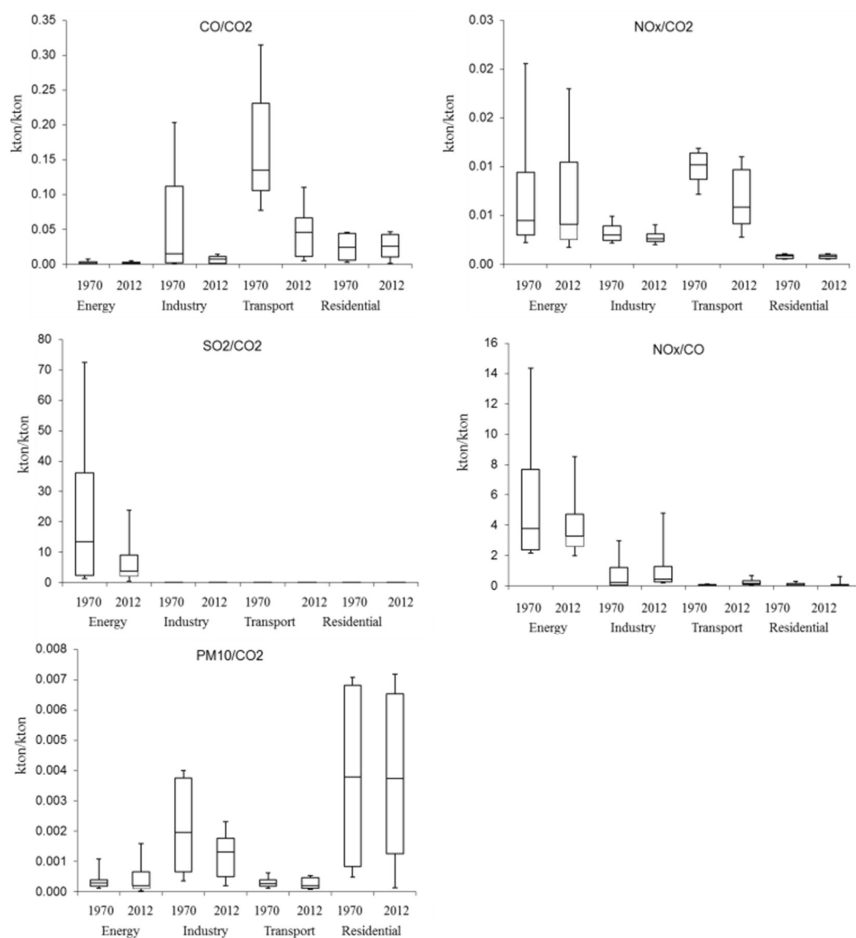


Figure 10 - Regional comparison of CO/CO₂, NO_x/CO₂ and SO₂/CO₂ emission ratios in 5 year time steps from 1970 to 2012 for all emitting sectors.



5 **Figure 11 – Comparison of 1970 and 2012 global emission ratios of CO/CO₂, NO_x/CO₂, SO₂/CO₂, NO_x/CO and PM₁₀/CO₂ (expressed in kton/kton) for different sectors. Box plots are calculated including all world countries and represent the 10°, 25°, 50°, 75° and 90° percentiles.**

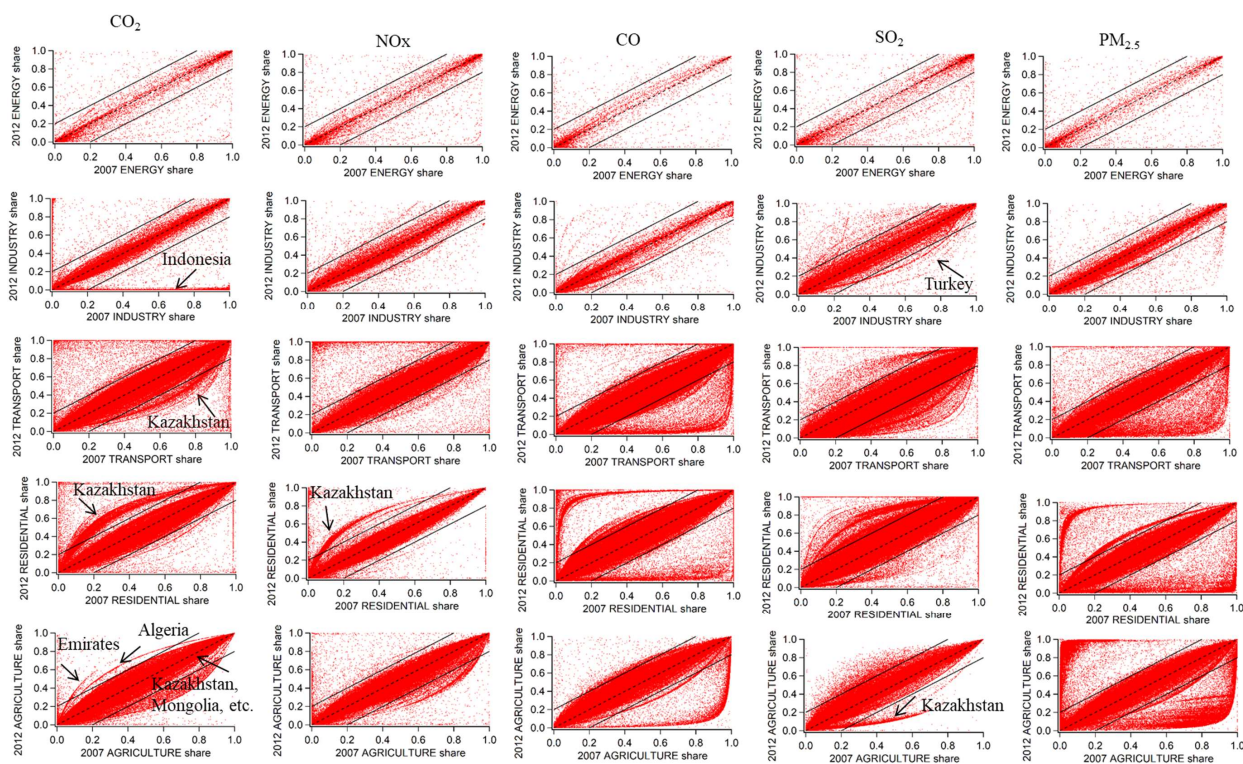


Figure 12 – Comparison between the 2012 and 2007 emission shares by sector at gridcell level for CO₂ (reference), NO_x, CO, SO₂ and PM_{2.5}.

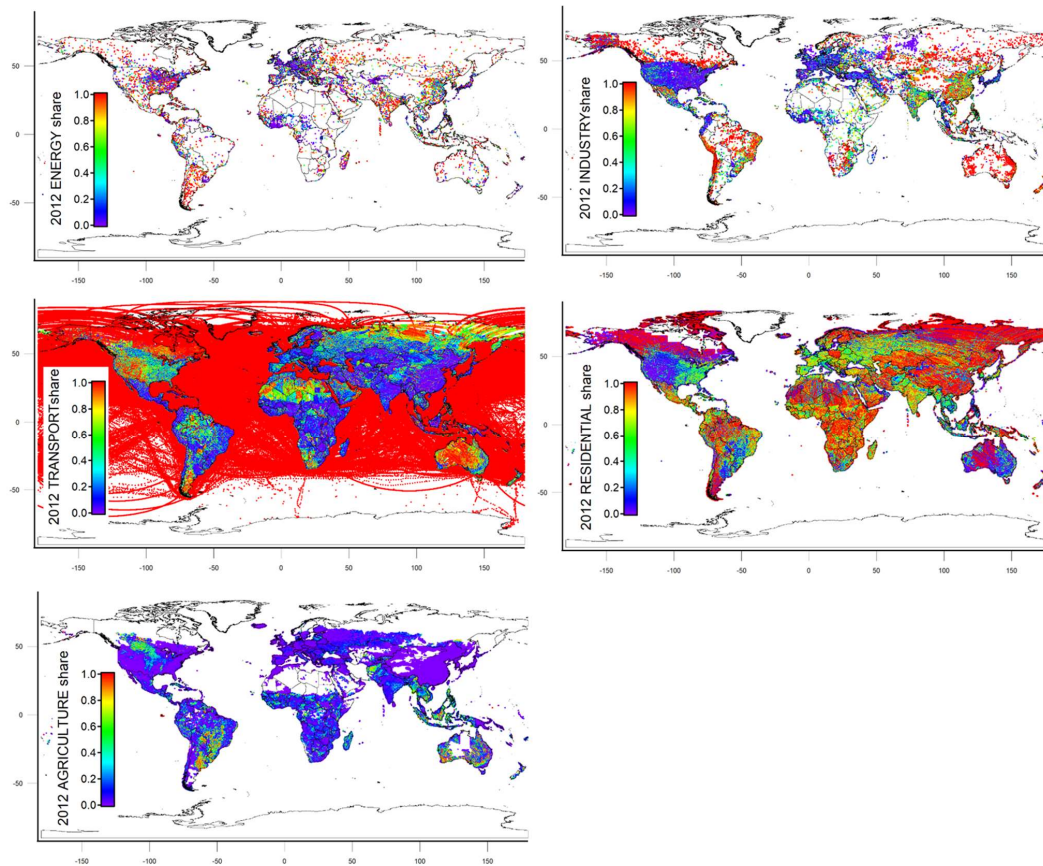


Figure 13 – SO₂ emission sector shares for the year 2012 at gridcell level.

5

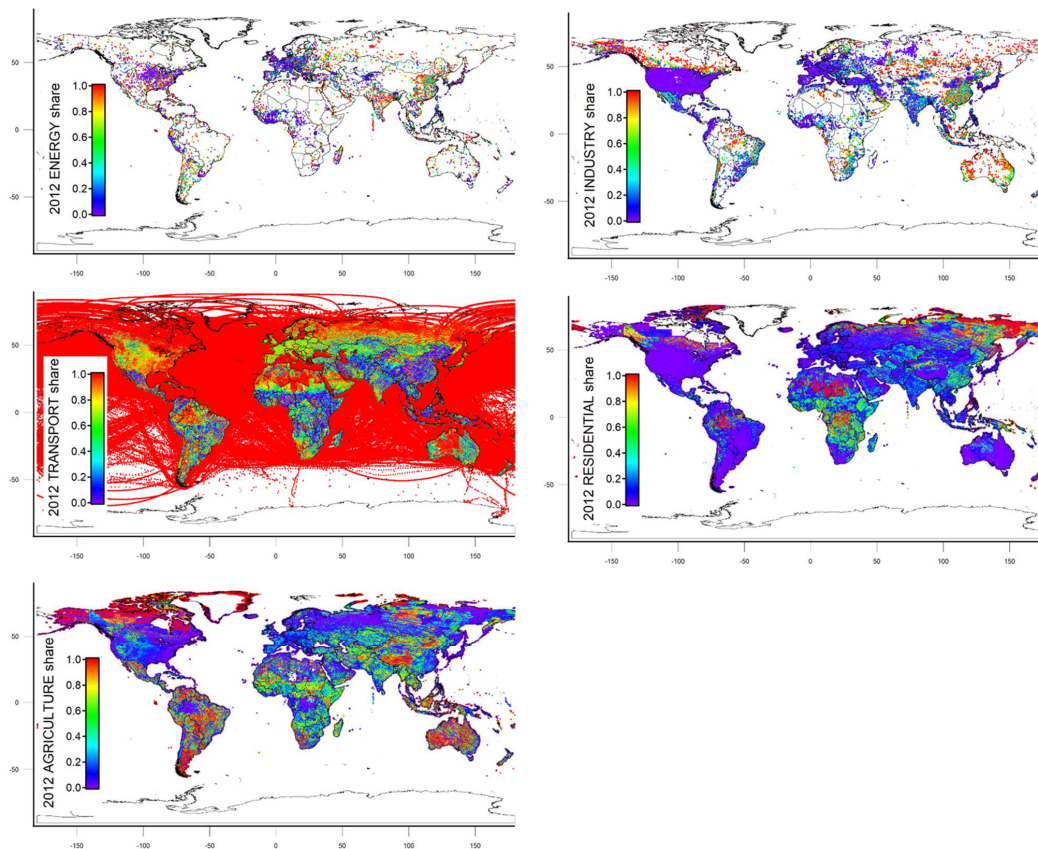


Figure 14 – NO_x emission sector shares for the year 2012 at gridcell level.

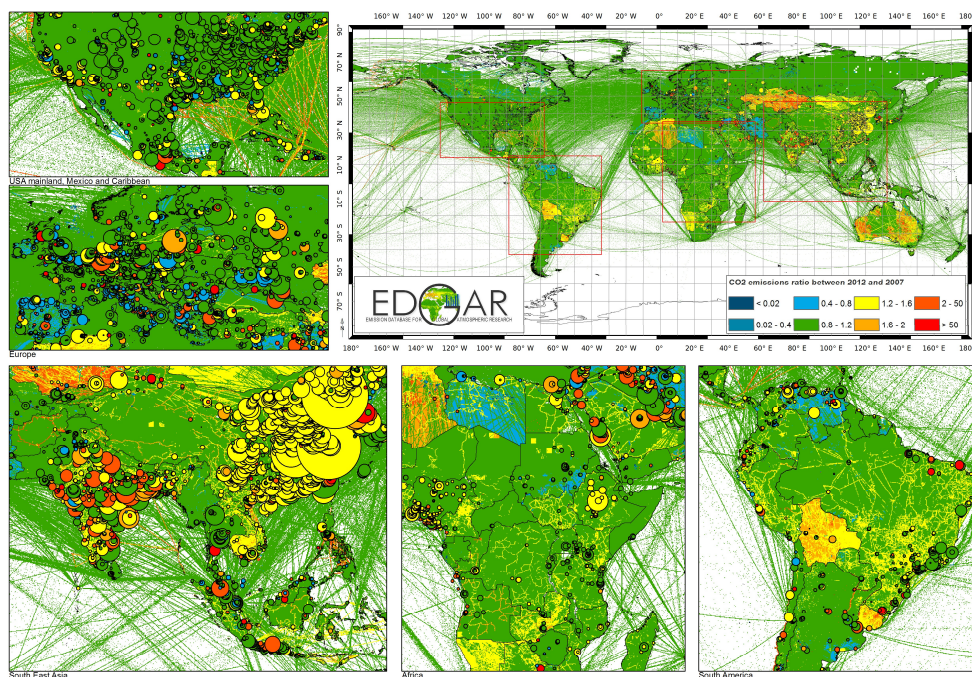


Figure 15a – Ratio of total CO₂ emissions, as proxy for activity, between 2012 and 2007 at gridcell level. The colored bubbles represent the top emitting cells, as described in the text.

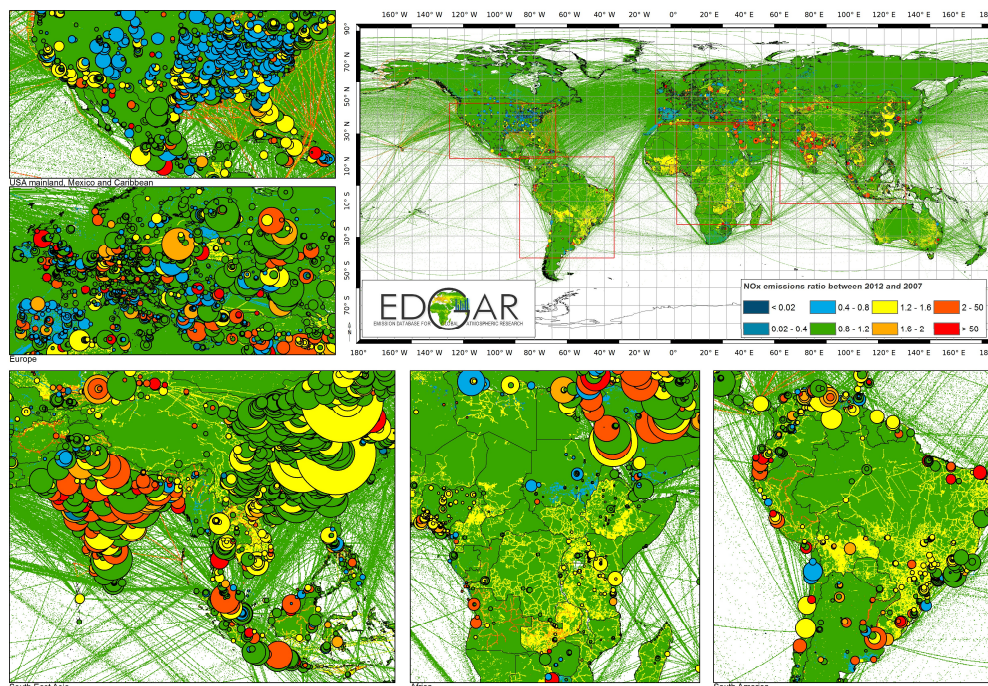


Figure 15b – Ratio of all sectors NO_x emissions between 2012 and 2007 at gridcell level. The colored bubbles represent the top emitting cells, as described in the text.

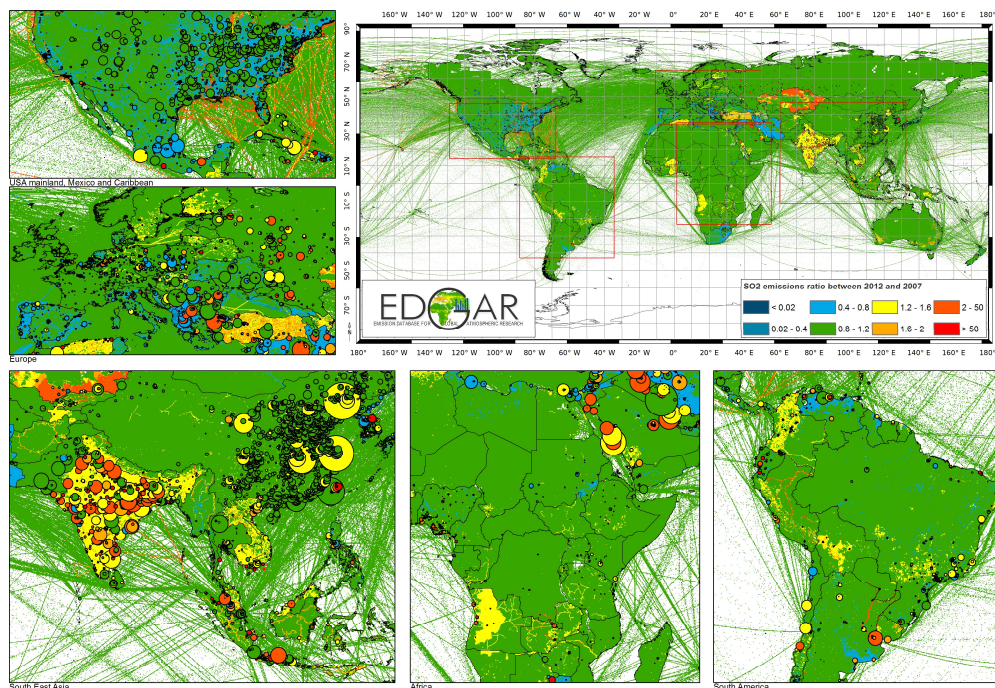


Figure 15c – Ratio of all sectors SO₂ emissions between 2012 and 2007 at gridcell level. The colored bubbles represent the top emitting cells, as described in the text.